A NEW LANE DETECTION SYSTEM FOR UNMANNED VEHICLES

by

Yasemin Timar

B.S, Computer Engineering, Middle East technical University, 1999

Submitted to the Institute for Graduate Studies in
Science and Engineering in partial fulfillment of
the requirements for the degree of
Master of Science

Graduate Program in Computer Engineering

Boğaziçi University

2010

A NEW LANE DETECTION SYSTEM FOR UNMANNED VEHICLES

APPROVED BY:

Associate Professor Fatih Alagöz .....
(Thesis Supervisor)

Professor Emin Anarım .....

Associate Professor Tuna Tuğcu .....

DATE OF APPROVAL: 17.09.2010

ACKNOWLEDGEMENTS

I would like to thank to my thesis supervisor Associate Professor Fatih Alagöz for his support and guidance during my thesis. I also would like to thank to Tuna Tuğcu and Emin Anarim who agreed to participate in my thesis committee.

I would like to express my grate indebtedness and love to my parents, my sisters and my brother for their continuous support, love, encouragement and confidence through my life.

I am all means grateful to my friends and colleagues in TÜBİTAK BTE for their precious comments and support.

I would like to thank to Evin Aslan and Gonca Gülbey who have revised my writing with an incredible patience.

ABSTRACT

A NEW LANE DETECTION SYSTEM FOR UNMANNED VEHICLES

As the intelligent transportation technologies have rapidly been improving, it is plausible to state that intelligent ground vehicles will be on the roads driving through the traffic in the near future. Moreover, intelligent vehicles will have a revolutionary effect in transportation industry, while eliminating accidents, and reducing the emission of carbon gases. Not only presently multiple intelligent vehicle projects are in progress in several countries but also the research and development departments of automobile manufacturers work on the traffic safety applications as well as autonomous navigation for future autonomous transportation. This study focuses on one of the most important traffic safety applications which is also a crucial part of a perception subsystem of an autonomous ground vehicle, that is, *Lane Detection*.

Main purpose of lane detection is to estimate the position of the road lane marks with a camera in order to calculate the distance to the lane and relative direction of the vehicle. Vision-based lane detection systems try to overcome the challenges of weather, lighting, road conditions to detect the lane marks. Within this thesis, we have proposed a novel lane detection method which produces successful results under challenging conditions. The method has three important phases; lane feature extraction, lane selection and road model fitting. The lane feature extraction method in our work is similar to the symmetrical local threshold. However, it is more powerful to detect eroded lane marks and road borders. In order to estimate the lane on the left and right side of the vehicle, Random Sample Consensus (RANSAC) algorithm fits a line with an error variance for lanes on both sides. Using the lane pixels on the estimated lines, a hyperbola-pair model is generated and the parameters of the road and the vehicle is calculated for the navigation subsystem. Results are presented on a reference image

database Road Marking database (ROMA) and evaluated with Receiver Operating Characteristic (ROC) and Dice Similarity Coefficient (DSC) curves. Synthetic images are also used to evaluate the performance of the lane detection technique.

ÖZET

İNSANSIZ ARAÇLAR İÇİN YENİ BİR ŞERİT TANIMA SİSTEMİ

Akıllı ulaşım teknolojilerinin hızla gelişmesiyle birlikte çok yakın bir gelecekte akıllı kara araçlarının trafikte seyrettiğini görmek mümkün olacaktr. Dahası insansız akıllı araçlar trafik kazalarını aza indirgeyerek ve karbon gazları salınımını azaltarak ulaşım endüstrisinde devrim niteliğinde bir etki yapacaklardır. Halihazırda bir kaç ülkede insansız kara aracı geliştirme projeleri devam etmekte ve bununla da kalmayıp otomobil üreticilerinin araştırma geliştirme bölümlerinde de trafik güvenlik sistemleri ve otonom ulaşım uygulamaları için otonom sürüş alanlarında çalışılmaktadır. Bu tez otomobilerde kullanılan trafik güvenliği sistemlerinin en önemlerinden biri olan ve aynı zamanda insansız kara araçlarının algılayıcı alt sisteminin kritik bir parçası olan *Şerit Tanıma* üzerine odaklanmıştır.

Şerit tanımanın esas amacı kamera görüntüsünde şeritlerin yerini belirleyerek, şeride olan uzaklık ile yol ve arabanını yönünün hesaplanmasını sağlamaktır. Bilgisayarla görme yeteneğine dayanan metodlar hava şartları, farklı aydınlanma koşulları ve yol şartlarının görüntü üzerinde neden olduğu problemleri çözmeye çalışmaktadır. Bu tez kapsamında hava ve yol durumunun zorlu şartlarında başarılı sonuçlar üreten yeni bir şerit tanıma metodu geliştirilmiştir. Metodun üç ana safhası bulunmaktadır; şerit özniteliklerini bulma, şeritleri ayrıştırma ve yol modelini oturtma. Bu çalışmadaki şerit özniteliklerini bulma yöntemi simetrik yerel eşik yöntemine dayanmaktadır, ancak silinmiş şeritleri ve yol kenarlarının bulunmasında çok daha başarılı çalışmaktadır. Aracın sağ ve sol yanındaki şeritlerin tanımlanması ve ayrıştırılması için RANSAC algoritması ile belirli bir hata varyansıyla her iki tarafta bir doğru denklemi tanımlanır. Doğru denklemini sağlayan pikseller kullanılarak en uygun hiperbol yol modeli ile yol ve aracın parametreleri hesaplanır. Geliştirilen metod ile üretilen sonuçlar yol imajları içeren

ROMA referans veritabanı üzerinde gösterilmiş ve ROC, DSC metrikleri grafik olarak sunulmuştur. Metodun başarısı ayrıca sentetik imajlar üzerinde de gösterilmiştir.

TABLE OF CONTENTS

LIST OF FIGURES

LIST OF TABLES

LIST OF SYMBOLS/ABBREVIATIONS

ADAS	Advances Driver Assistance System
DLT	Direct Linear Transformation
DSC	Dice Similarity Coefficient
DGPS	Differential Global Positioning System
GPS	Global Positioning System
IPM	Inverse Perspective Mapping
ITS	Intelligent Transportation Systems
LIDAR	Light Detection and Ranging
PID	Proportional Integral Derivative
RANSAC	Random Sample Consensus
ROMA	Road Marking Database
ROC	Receiver Operating Characteristic
UGV	Unmanned Ground Vehicle
VIAC	Vislab Intercontinental Autonomous Challenge

1. INTRODUCTION

Increasing the traffic safety has been an active research topic for decades. United Nations (UN) has reported that each year 1.3 million people are killed and at least 50 million are injured in traffic accidents worldwide. Within the recent UN campaign known as Decade of Action for Road Safety 2011-2020, four fundamental development areas have been emphasized to attain 50% reduction in the number of people killed in traffic accidents[1]. These areas are listed as;

- Safer vehicles
- Safer roads,
- Vaccines for road safety
- Mobile international support.

Ultimate goal for future public transportation would be to build safer roads and intelligent vehicles which can accomplish transportation purposes while avoiding accidents without or with a little human assistance. Moreover intelligent vehicles will have a revolutionary effect in transportation which will transform the industry while virtually eliminating accidents, and reducing the emission of carbon gases.

Intelligent transportation systems cover internetworking, communication and controlling frameworks for monitoring and collecting accurate traffic and environment information to improve road safety. In-vehicle technologies like airbags, crash zones, ABS braking system are just a few of the safety functions commonly used. On the other hand, GPS, RADAR, LIDAR, camera and other sensors with various navigation tools and computer vision applications are developed to be used to control the vehicle according to regulations and avoid collisions. Some of the traffic safety applications developed for vehicles can be listed as follows;

- Lane Departure Warning Systems
- Adaptive Cruise Control

- Driver Attention Monitoring
- Obstacle Detection and Warning
- Autonomous Vehicle Control

This thesis concentrates on lane detection, which is crucial for all those systems. Road following, lane keeping performance are dependent on road lane marks, which can be described as visual signs painted on the road. Most of the lane detection systems which have been developed are vision based, since lane marks can not be easily detected by any sensor other than a camera. We have examined several types of lane detection methods and proposed an alternative technique which has lower complexity and higher robustness to shadows, lighting changes, erosion and occlusion. The proposed methods can easily be integrated to an advanced driver assistance system (ADAS) or an autonomous vehicle navigation system.

Unmanned ground vehicles are (UGV) described as robotic platforms operating outdoors and over a wide variety of terrain. In this study we use the term unmanned vehicles referring to driverless cars sometimes called intelligent vehicles which are autonomous and operate by themselves without any driver assistance.

1.1. Problem Definition

Road lane mark detection depends on the fact that marks are painted with colors of white or yellow on dark-colored roads. However, due to light changes, weather conditions and erosion it becomes more difficult detect the road marks. Conditions that the road markings may not be clearly visible during navigation are described as [2];

- Variable lighting conditions, such as bright sun, or cloudy weather
- Shadows of trees, vehicles, overpasses
- Variable scene content, from dense urban to the countryside
- Variable road types, such as highways, main road, back country road

Designing a successful system functioning in those conditions is still an ongoing research topic since each condition has its own difficulties.

It is also necessary to model road and lane marks according to the vehicle for accurate localization. Vehicle lateral position which can be defined as the distance to the left lane to be calculated to evaluate lane keeping performance. Road curvature is also an important factor related with vehicle direction and road following. Lane models which take curvatures into account will produce more accurate results to control a vehicle.

The perception subsystem of an autonomous vehicle should respond in the time interval which the planning and motion planner can respond to incoming data as soon as possible. Real-time road image processing is dependent on the algorithm executed on the image. Implementing such an algorithm with less error rate is a challenge for a lane detection system. Image processing techniques with less complexity will outperform in this challenge.

1.2. Objectives & Scope

Development of an intelligent vehicle involves implementing subsystems from various disciplines. Four main subsystems can be defined as;

- Vehicle Control
- Path Planning
- Environment Sensing
- State Estimation and Localization

Vehicle control system is generally implemented by actuators and motion controllers, whereas path planning and reasoning algorithms are implemented with various artificial intelligence techniques. Several types of sensors are integrated to the vehicle for environment sensing. Monocular cameras are very popular to be used for road and obstacle detection, whereas laser range finders are also installed for collision detection.

As a result, environment model is produced by processing the sensor information. State estimation and localization process environment information with tracking methods to evaluate target velocity and direction of the vehicle.

Designing and building such an integrated system has been an active research area more than thirty years. Along with the recent technological developments in automotive industry and computer science, cost of building an autonomous vehicle is much cheaper than it was.

This thesis is a part of the idea of implementing an intelligent vehicle project using local resources. Although the vehicle does not exist, lane detection system can still be implemented and easily integrated to a perception subsystem of an autonomous vehicle. Since there is no test-bed for implementing the lane system presented in this thesis, calibrated images from ROad MArking road image database have been used to produce the results. Experimental results are also presented on videos from a webcam mounted on an automobile driven in campus ground.

1.3. Contributions

Within this work, an alternative approach to lane detection is proposed. Robust feature extraction modules with efficient lane models are integrated in a novel way. The complexity of the algorithm is much less than any other edge-based or texture-based lane extraction systems. Still the system has the advantages of hyperbola-pair lane model in that it is capable of functioning in different light conditions, in different road types, with different image resolutions and with different types of lane marks.

The proposed lane detection system is robust to strong shadows, eroded lane marks and curvatures. The method uses Random Sample Consensus (RANSAC)[3],[4] technique for the selection of lane pixels forming a regular shape. This approach is different from the other methods which use Hough transform or template matching. The distribution of lane candidates is the main clue for the detection of the lane region, and it doesn't use any training phase or template to fit a model. Method

successfully works on road images with strong shadows and eroded markings. System also produces promising results on images with obstacles or occlusions. Each frame is processed independently to form a base for a future work of tracking system.

The lane detection system implemented within this thesis overcomes the difficulties caused by various road and light conditions. Easily being integrated into a perception subsystem, the system can be used under many road conditions in which an autonomous vehicle is driving.

1.4. System Overview

The proposed system includes three main functional phases, which are summarized in Figure 1.1. Each image from the camera is processed to extract candidate pixels of a lane or road border which is defined as the lane feature extraction. The lane extraction method is based on local thresholding which is very effective in various light conditions. After lane feature extraction phase, candidate pixels which fit to a line model within a given error variance are selected to be a lane or road border pixel using RANSAC. Left and right lanes are separated by estimating the left and right regions of image coordinates. And finally, in order to estimate road and vehicle parameters, the lane pixels are modeled as a hyperbola pair defined by road, vehicle and camera parameters [5],[6].

1.5. Thesis Outline

Chapter 2 includes a survey of the different intelligent vehicle research projects. The main modules of an intelligent vehicle and their relation is explained in subchapters. Chapter 3 provides a literature review on lane detection and modeling. Various types of lane extraction methods are reviewed and evaluation methods of lane extraction techniques are explained. Different techniques like IPM and DLT for perspective removal are reviewed in the sections 3.5 and 3.6 respectively. Proposed lane detection method is explained in chapter 4. Main modules of our method Lane Feature Extraction and Lane Selection are discussed in section 4.1 , Lane Model is explained

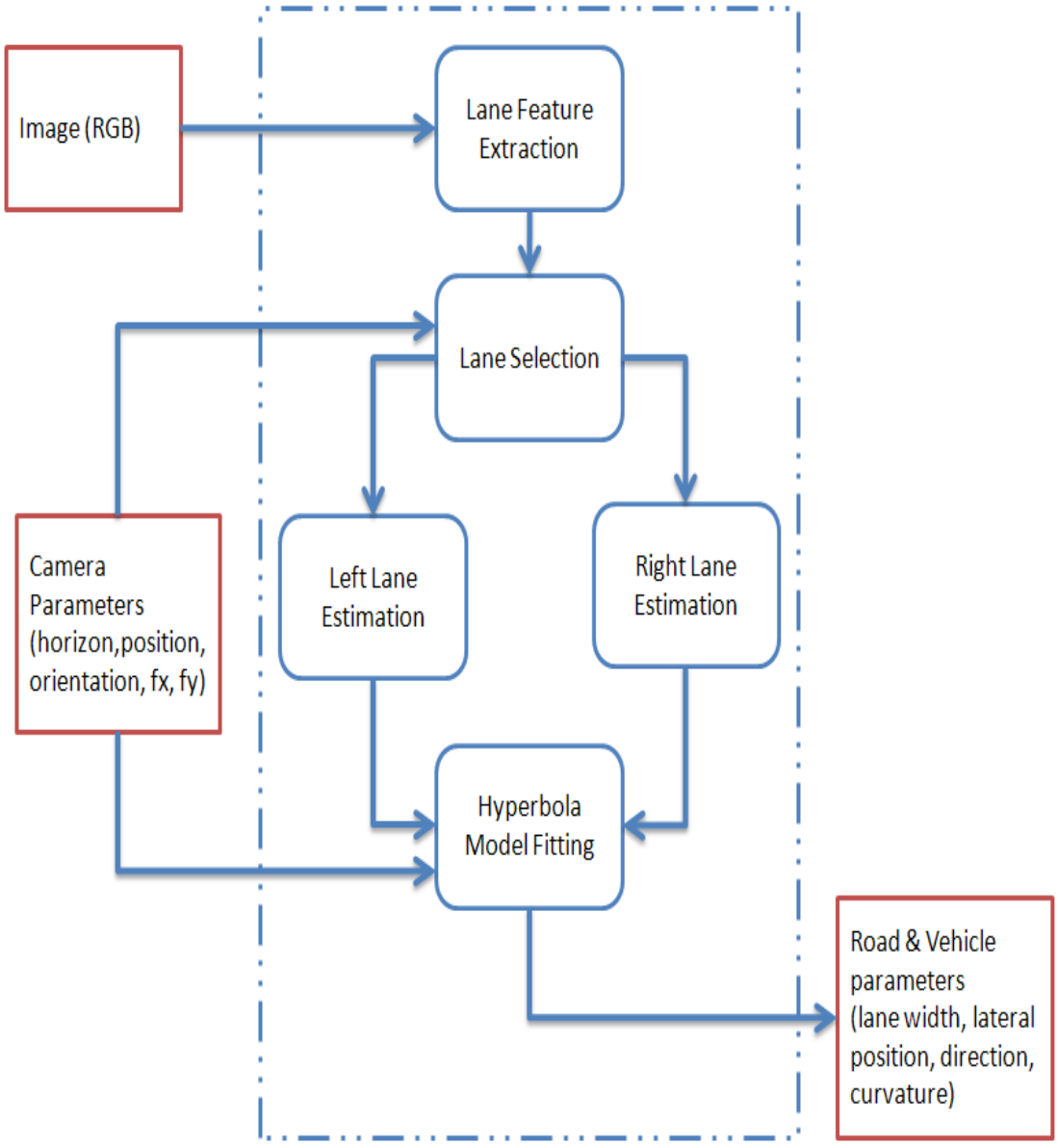

Figure 1.1. System Overview

in sections 4.2 and 4.3. Results and performance measures are presented in the last chapter 5. We cite possible future works that might proceed this study.

2. INTELLIGENT VEHICLES

Intelligent vehicles play the major role in Intelligent Transportation Systems (ITS) while using sensing, communication, computing and control technologies to understand driving states and environments for the purpose of assisting vehicular operations, traffic control, service management, and many other activities.[7]. It has been more than thirty years since intelligent transportation systems technologies became a research topic to solve the problem of transportation of people and goods[8]. With the collaboration of universities, automobile manufacturers and research centers in different countries, there has been various intelligent vehicle projects all over the world.

The project initiated in Europe known as the PROgraM for a European Traffic system with Highest Efficiency and Unprecented Safety (PROMETHEUS) is the first large scale consortium involving 19 European countries with 13 vehicle manufacturers, several government research centers and a variety of universities gathered in early 1986 for developing ITS technologies [8]. As a part of EUREKA Prometheus Project the robot vehicles VaMP and Vita-2 are constructed by Daimler-Benz and Ernst Dickmanns [9].The VaMP driverless car was one of the first truly autonomous cars along with its twin vehicle, the VITA-2. They were able to drive in heavy traffic for long distances without human intervention, using computer vision to recognize rapidly moving obstacles such as other cars, and automatically avoid and pass them [9].

The National Automated Highway System Consortium (NAHSC) was funded in United States in 1995. Like the PROMETHEUS project, it contained a number of universities, research centers and automobile manufacturers across America [8]. Today the NAHSC is no longer being funded by US Congress. However first road-following demonstration with laser-radar and autonomous robotic control in United States is accomplished with Autonomous Land Vehicle (ALV) funded by Defense Advanced Research Projects Agency (DARPA).

Figure 2.1. Boss, Tartan Racing robot in DARPA Urban Challenge

In 2002, the DARPA Grand Challenge competitions were announced. The 2004 and 2005 DARPA competitions allowed international teams to compete in fully autonomous vehicle races over rough unpaved terrain and in a non-populated suburban setting. The 2007 DARPA challenge, the DARPA urban challenge, involved autonomous cars driving in an urban setting. First two challenges took place in off-road desert environments. However, in the last challenge vehicles must navigate an ordered list of checkpoints in a road network in an urban area and must obey traffic laws while driving, merging or splitting in traffic, negotiating busy intersections, avoiding obstacles in a limited time. The winner of the Urban challenge, The Boss build by Carnegie Mellon University Navlab in association with General Motors, Caterpillar and Continental AG is presented in Figure 2.1. In 2008, General Motors stated that they will begin testing driverless cars by 2015, and that they could be on the road by 2018.

From 1996-2001, Prof. Alberto Broggi of the University of Parma organized the ARGO Project, which worked on enabling a modified Lancia Thema to follow the normal lane marks in an unmodified highway with an average speed of 90 km/h. 94% of the time the car was in fully automatic mode, with the longest automatic stretch being 54 km. With only two monocular low-cost video cameras on board, stereoscopic vision algorithms are used to understand the environment. ARGO Project worked

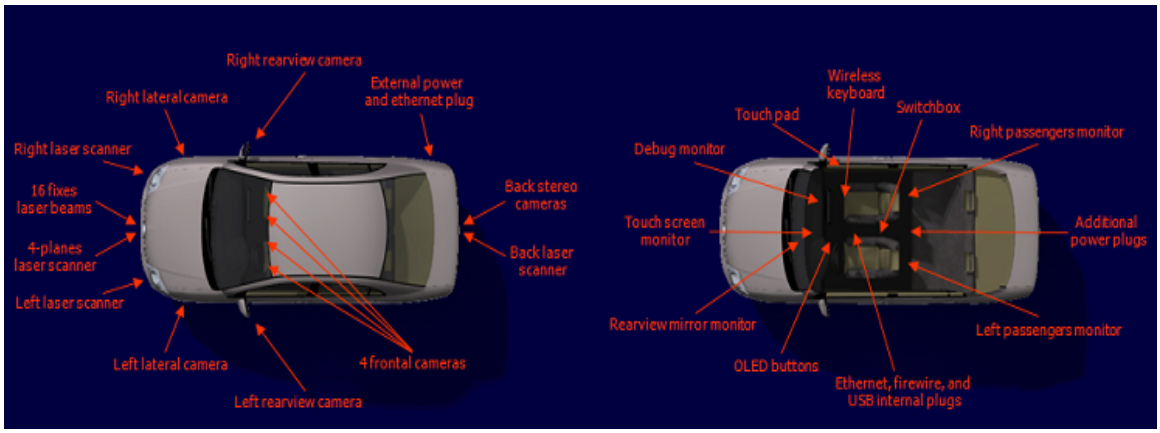

Figure 2.2. BRAiVE External and Internal Equipment

on a modified Lancia Thema to make it autonomously follow the normal (painted) lane marks in an unmodified highway. The vehicle had only two black-and-white low-cost video cameras on board, and used stereoscopic vision algorithms[10]. The ARGO vehicle was followed by BRain-drIVE (BRAiVE) vehicle; ARGO was developed in 1996 and demonstrated to the world in 1998; BRAiVE in Figure 2.2 was developed on 2008 and firstly demonstrated in 2009. BRAiVE is introduced as a prototype vehicle which was designed to serve as a test-bed for innovative concepts integrating several numbers of sensors with human machine interfaces. BRAiVE has been also used to collect ground truth data for ADAS applications.

The latest project of Prof. Alberto Broggi and his research team in VisLab is The Vislab Intercontinental Autonomous Challenge (VIAC) in which autonomous vehicles are being prepared and tested to drive with no human intervention from Parma, Italy to Shangai, China along a 13,000 km and three months unique journey. Main motivation of the challenge is to test and stress their technology on a long and extreme (including all sort of traffic, weather conditions, road infrastructures, and even off-road) route to asses the performance of the system.

2.1. Overview

Unmanned vehicle platforms range from small sized four-wheeled platforms to huge transportation trucks. Recent types of automobiles which has drive-by-wire sys-

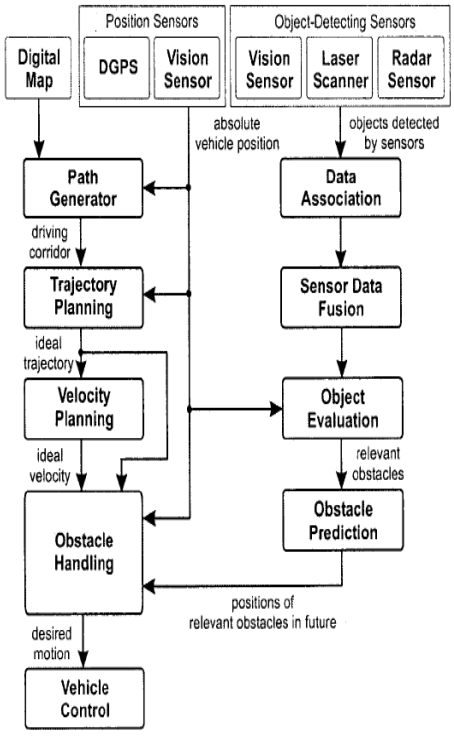

Figure 2.3. Vehicle guidance system architecture proposed by Simon & Becker

tems can be converted to an autonomous vehicle just like "Junior"[11] which is developed by Stanford Racing Team for DARPA Urban Challenge. Various system architectures have been proposed for vehicle guidance and control. Two examples are presented to introduce the main subsystems of an intelligent vehicle. The system proposed by Simon & Becker in 1999 is given in Figure 2.3. The system architecture of Tartan Racing team intelligent vehicle Boss is presented in Figure 2.4[12]. As the reader can see several subsystems are designed to operate for different goals of autonomous driving. The four subsystems we have mentioned exist in both them but with different names.

Within this work, we are mainly interested in the sensor system of the intelligent vehicle with its connection with the control system specifically for lane detection. We focus on the perception systems and examine in the technical reports of the participated teams.

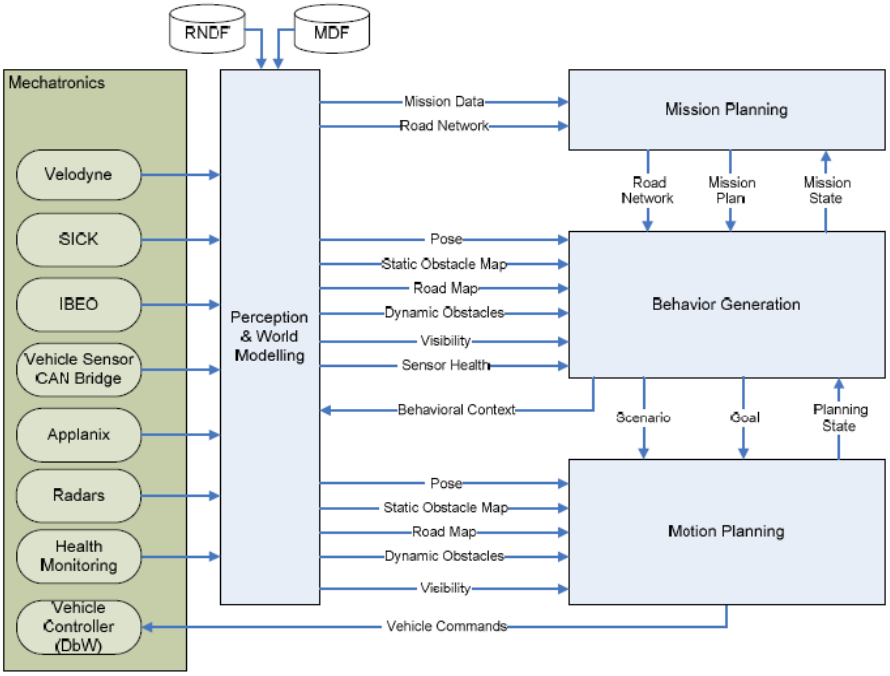

Figure 2.4. System architecture of The Tartan Racing robot in DARPA Urban Challenge

2.2. Mission Planning

The route to the destination is computed by a planning algorithm using digital maps and other electronic route data. Artificial intelligence algorithms are executed in order to reason about the optimal path to reach the destination much like a human driver [12]. The mission planner compares routes based on prior knowledge of congestion or blockages, construction, and the legal speed limit. Current GPS systems, navigation products are used in mission planing modules. DGPS is also used where it is available.

2.3. Motion Planning

Motion planner of an intelligent vehicle consists of three main subsystems. One of them plans and keeps the trajectory of roads, which are parts of the path leading to the destination. Avoiding static and dynamic obstacles (pedestrians, other vehicles, static objects, etc.) is the other subsystem. Keeping the vehicle in the desired state

with the desired velocity is also achieved by the motion planner of the vehicle. These functions process the environment information to execute planning algorithms.

2.4. Vehicle Control

Main components of a ground vehicle to be controlled are the steering, throttle, brake and gear shift. Motion controllers like PID controllers generate steering and velocity controls that are executed by the vehicle. Desired trajectories produced by the path planner are inputs of the motion controllers. Additionally, path planner computes desired speed of the vehicle. With desired trajectory and speed information, steering controller minimizes lateral offset of the vehicle to the desired trajectory while the velocity controller arranges brake pressure and throttle position to reach at the desired velocity.

2.5. Environment Sensing

Different types of sensors have been used in intelligent vehicles. Main categorization of sensors are defined according to their ranges. The long-range sensors are used to sense the region in front of the vehicle that is generally located in either the horizontal or vertical planes. Terrain, obstacles, roads, or other vehicles are detected within long-range. At moderate or high speeds, the data from the long range sensors are processed in time to make changes in the heading and/or speed of the vehicle either to avoid the obstacle or to switch to a slow speed for obstacle avoidance. The short-range sensors are used to sense regions to the sides and rear of the vehicle as well as in the front. They provide input for obstacle avoidance-path planning as the vehicle moves at low speeds [13]. The general characteristics of each of the sensors are summarized below.

- Video camera: Generally monocular video cameras with moderate resolution (640x480 or 320x240) are primarily used as short-range/long-range sensors for detecting the edges of the road/trail and other vehicles in the forward direction. Their sensing horizon depends on the visibility and how they are aimed. A maximum sensing distance of up to 100 m will be achievable on flat straight paths.

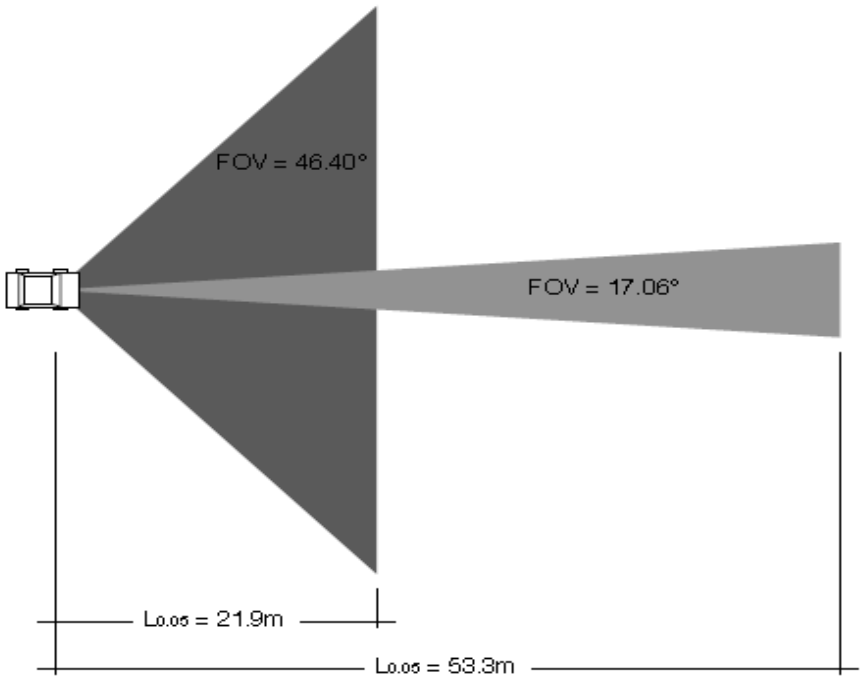

Figure 2.5. S

hort/long range cameras with different field of view in CeDAR[14]

- LADAR/LIDAR: The purpose of LADAR system is primarily detecting obstacles, other vehicle and terrain contour at large distances in front of the vehicle. It has the capability of detecting targets at a maximum range of 80 m with a range resolution of 0.3 m. An infrared laser beam is mechanically scanned over an angular range.
- RADAR: The RADAR system is used, primarily for detecting obstacles at large distances in front of the vehicle. It is capable of detecting targets at a maximum range of 110 m with a range resolution of 1 m. The RADAR supplements the obstacle detection capability of the LADAR system in situations where visibility is limited by dust, fog, or rain. It will also be relied upon when the LADAR system is "dazzled" by the sun.
- Ultrasonic sensor: The ultrasonic range finder will be primarily used for detecting obstacles at short distances on the sides, in front of the vehicle, and to the rear of the vehicle. It will rely on the diffuse reflection of ultrasonic waves from obstacles. Its maximum usable range is estimated to be 9-10 m.

- Photoelectric sensors: Depending on the specific methods employed for installation of the photoelectric sensors, they provide information about the presence, approximate range and location in combination, or only about the presence of the obstacle and a rough idea of the general location around the vehicle. Time modulation of the LED light sources allows the sensors to operate in the presence of considerable external light. Their maximum usable range is 5-6 m.
- Tactile: Flexible bumper tactile sensors detect contact with objects at around 8 inches around the vehicle. They use a combination of electro-mechanical microswitches, and/or interruption of self-contained low power light circuits to detect bumper motion in response to pressure contact.
- GPS/DGPS: GPS generally includes a single antenna and receiver to generate unbiased measurements of position (north and east), velocity (north, east, up coordinates) and course.

Data from various sensors are processed to produce the environmental model which the other subsystem algorithms use. Obstacles, traffic signs, lane marks are detected in the world coordinates and static and dynamic obstacle maps are generated. Several sensors and their capabilities for intelligent vehicles are listed in the following table.

Vision-based lane detection systems generally utilize monocular cameras. Next chapter discusses the various techniques proposed in the literature.

Table 2.1. Sensor types integrated in intelligent vehicles

Sensor	Active/Passive	Primary Purpose
Stereo camera pair	Passive	Range detection of obstacles, roads, terrain, other vehicles
Single camera	Passive	Detection of obstacles, roads, lanes, terrain, other vehicles
LADAR (LIDAR)	Active	Obstacle avoidance & terrain classification
RADAR	Active	Obstacle avoidance within long range
Ultrasonic distance sensor	Active	Obstacle avoidance
Photoelectric sensors	Active	Obstacle avoidance
Tactile sensors	Passive	Detection contact with objects

3. LANE DETECTION LITERATURE

According to recent surveys on lane detection methods, it is reported that namely all lane-position-tracking algorithms involve similar processing units[15]. A broad survey on vision-based lane detection and tracking is presented in [15] in which techniques are listed and categorized according to their main modules. As it is given in Figure 3.1, main modules are road/lane feature extraction module, road and vehicle model, postprocessing methods and estimation of vehicle and road model with time.

Proposed lane detection systems in literature include various algorithms which are region-based [16],[17], edge-based [18], gradient-based [19],[20],[21], ridge-based[6], intensity-based [22],[23] techniques. Region-based lane detection methods are time-consuming and inaccurate due to various textures on roads and changing colors caused by illumination changes [24]. Methods based on edges and gradients and intensities are affected by shadows and obstacles in the images [24]. Strong shadows, many extraneous lines, eroded markings and high curvatures are still ongoing issues to be solved in lane detection. Recent works on evaluating various lane feature extraction techniques give detailed comparison with numerical results [2]. In section 3.1, those approaches will be explained in detail.

Road model is integrated with lane feature extraction in various techniques. Methods based on line models are successful on highway roads. With Inverse Perspective Mapping (IPM)[10], perspective effect on the image is removed and road lanes are modeled as parallel lines with fixed width in Generic Obstacle and Lane Detection (GOLD) system [21]. Hough transform has been widely used to model lanes as straight lines [15]. To represent curved roads several other models like deformable template models [24], high degree polynomials, cubic splines [25], clothoids, parabolas are proposed. General assumptions in various road models are; (1) road is flat, (2) curvature is constant. Hyperbolic road model in the work of [5] with the fact that lanes can be modeled with two hyperbolas parallel to each other enables us to estimate the width of the lane, vehicle lateral position, vehicle direction and road curvature information

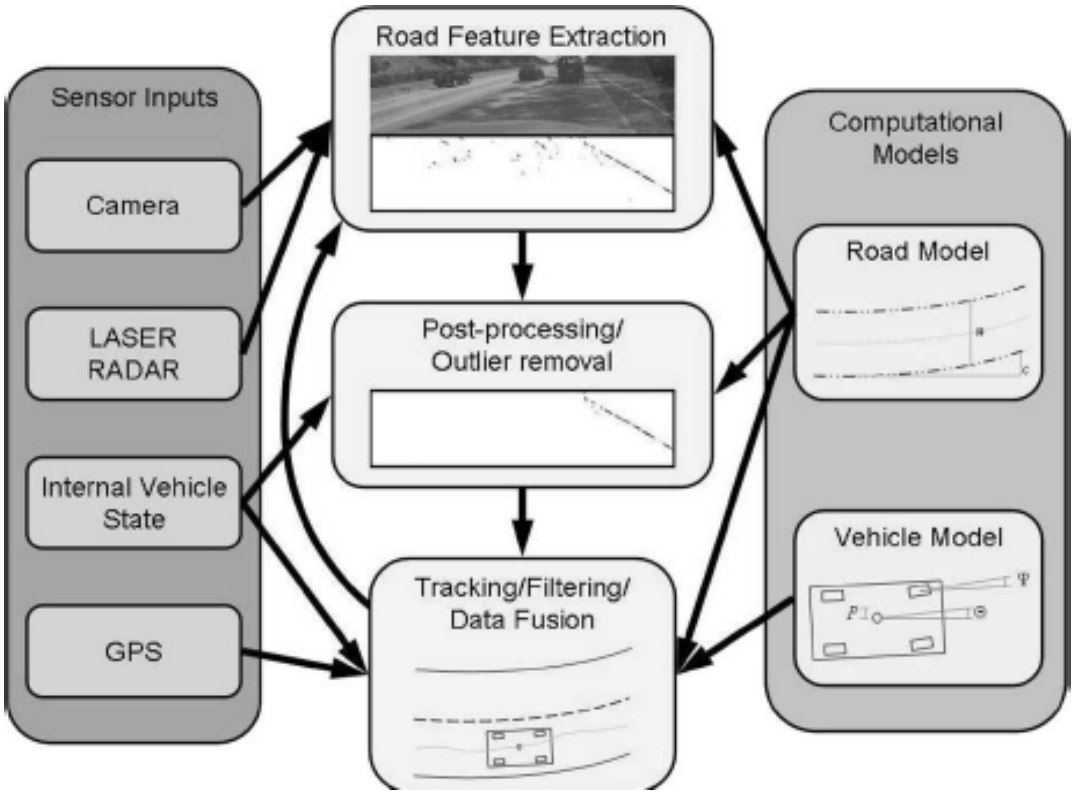

Figure 3.1. Generalized flow chart for lane-detection systems

[6].In section 3.1. these approaches will be explained in detail.

Postprocessing is necessary for improvement of extracted lane features and road estimation. Hough transform is a common technique for post processing presented in Figure 3.1. Features based on orientation or likelihood [26] are enhanced in other methods.Multiple cues proposed in [27] are scheduled to be processed to determine which feature should be extracted and fed-into position-tracking module. Tracking lanes enables the system to estimate the location and orientation of lanes before extraction. Kalman Filter and particle filter have been used for tracking in most of the temporal lane-position detection systems.

3.1. Lane Feature Extraction

Lane feature extraction is the first and the most important part of lane detection. Most of lane detection techniques have been executed on gray scale images to detect edges [26][28]. Transforming the image into a top view perspective was introduced

with GOLD system [21]. Morphological filters [21], steerable filters [29] and histogram analysis [30] are some of the methods used for feature detection. Lane model is also the most important part of the detection system. Methods using Hough transform represent the left and right lane marks as single lines. Lanes are also modeled as concentric circular arcs [26] and B-Snakes [31].

In their recent paper which is presented in Conference on Intelligent Transportation Systems, October 12-15, 2008, "Evaluation of Road Marking Feature Extraction" [2], authors propose a systematic approach to evaluate algorithms for extracting lane marks features. Main extractors that are compared are geometric selection and photometric selection based techniques and it is restricted to process single frames. For evaluation, six algorithms have been chosen to be compared on the data set which is prepared by the authors and shared for research purposes. The data set ROMA, a reference database containing over 100 images of natural road scenes with corresponding manually labeled ground truth images, is presented for the use of evaluating and comparing lane mark extractors. Within the database camera calibration and horizon information which is used for outlining are available for each image. As it is stated in the paper colored image processing is very similar to the gray scale image processing for the extraction algorithms in the procedural manner. However complexity increases in colored images. And it is advised that "...when maximum speed is a strong requirement, gray level images can be used with a slight loss in terms of performance." [2]. According to this advice it is preferred to process gray scale images in our techniques.

Evaluation of road marking detection algorithm is dependent on the size, shape, position match between the resulting marker detection with the expected marker detection on the original frame. It is proposed in [4] to use Receiver Operating Characteristic (ROC) curves to compare the different techniques. On the other hand, algorithms are expected to depend on a threshold value of intensity, probability, etc. In this work ROC curves are also utilized. As long as the ground truth image is available for all the frames, TPR (True Positive Rate) and FPR (False Positive Rate) is computed by simple comparison of each pixel in the ground truth image versus the resulting threshold image. Below are two ROC curves resulting from two versions of the global threshold

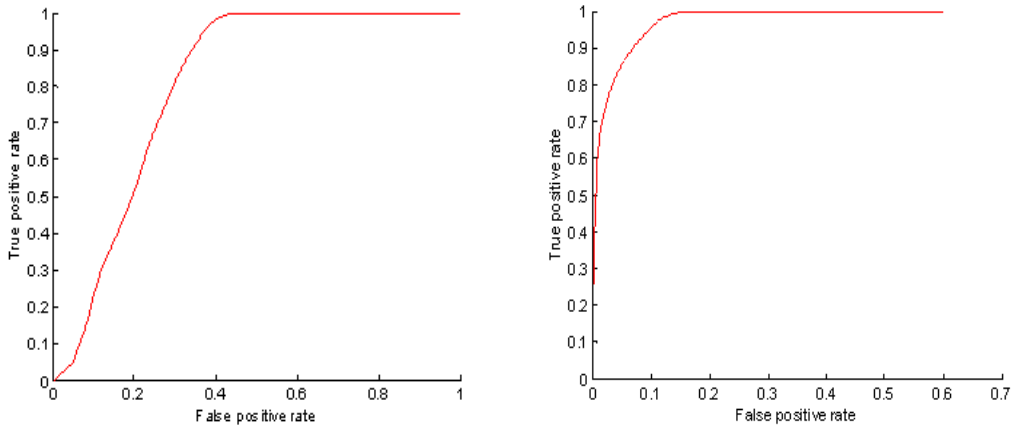

Figure 3.2. ROC curves of global threshold method with and without horizon information

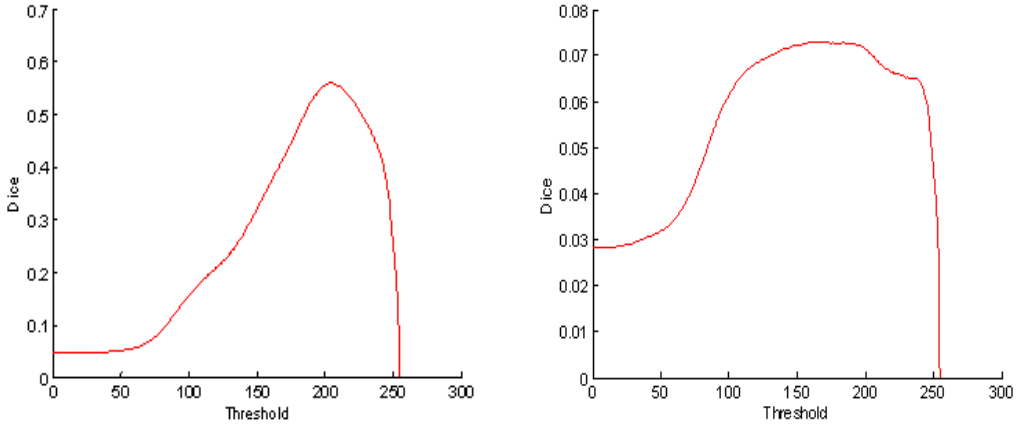

Figure 3.3. DSC curves of global threshold method with and without horizon information

algorithm. Left one discards the information above the horizon line, the other is the result of processing all the pixels.

The area under the ROC curve presents the performance of the algorithm. In other words, the bigger area shows better performance. When the horizon information is available, there is a huge improvement in the results. Another tool to evaluate the algorithms has been defined to be Dice Similarity Coefficient (DSC) as proposed in [2]. The DSC penalizes the False Positives (FP) which is good for detecting small sized

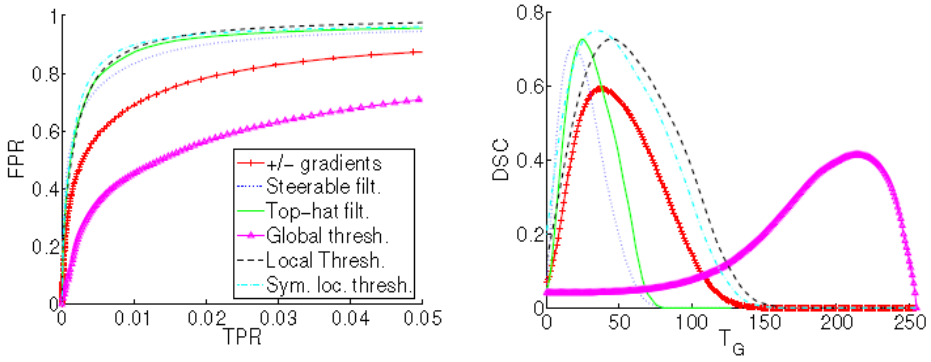

Figure 3.4. ROC and DSC curves for 6 algorithms on ROMA database [2]

markings. DSC is defined as;

$$DSC = \frac{2TP}{(TP + FP) + P} \tag{3.1}$$

The maximum value of DSC curve is related to the optimal value of threshold. Since ROC and DSC curves have been used to evaluate different extraction algorithms, we will use this measure to evaluate the lane extraction performance of our system.

Veit et al. compared some of the lane extraction methods in their valuable work [2]. They have pointed out that photometric and colorimetric features with just a minimal geometric selection should be selected for lane extraction. At the end there is still no single method without problems. They have chosen local threshold method, which produces very good results on the whole database. However, it does not provide the optimal results with high curvature. Still the method has the advantage of implementation simplicity with less computation complexity.

Out-door images have adverse lighting changes caused by sun, clouds and shadows of surroundings. The texture of the road (eroded marking, tar, etc.) and natural environment create a broad range of colors in natural road scenes. These issues are still addressed in lane extraction.

In this work we will categorize the road feature extractors according to the feature they depend on; however, we will not differentiate them as geometric or photometric

as they are categorized by Veit et al. in [2].

3.1.1. Gradient\Edge Based Methods

As [14] has clearly stated that the basic assumptions of the road lane marks supports to use gradient based feature extractions; (1) gradient methods are invariant to brightness intensity levels, (2)structure roads have well-defined edges or lane marks, (3) a transition between the road and surroundings will induce gradient image space.

Methods based on gradient and edge extraction have been commonly used in lane extraction literature[26][21]Edge detection techniques are generally based on Gaussian gradient or a similar filter convolution. Image I is convolved with a kernel f and x_i and y_i are unit vector in image coordinates, $*$ is convolution operation in 3.2

$$\triangle I = \frac{\partial I}{\partial x} i_x + \frac{\partial I}{\partial y} i_y = (f_x * I) i_x + (f_y * I) i_y \tag{3.2}$$

Common kernels like Sobel and Prewitt are given in 3.3 and 3.4. The weights of the neighbors are different in Sobel kernels and Prewitt uses equal weights .

$$f_x = \frac{1}{4} \begin{bmatrix} 1 & 0 & -1 \\ 2 & 0 & -2 \\ 1 & 0 & -1 \end{bmatrix}, f_y = \frac{1}{4} \begin{bmatrix} 1 & 2 & 1 \\ 0 & 0 & 0 \\ -1 & -2 & -1 \end{bmatrix} \tag{3.3}$$

$$f_x = \frac{1}{3}\begin{bmatrix} 1 & 0 & -1 \\ 1 & 0 & -1 \\ 1 & 0 & -1 \end{bmatrix}, f_y = \frac{1}{3}\begin{bmatrix} 1 & 1 & 1 \\ 0 & 0 & 0 \\ -1 & -1 & -1 \end{bmatrix} \tag{3.4}$$

One dimensional kernels are also used in images. Some of them can be defined as follows;

$$f_x = f_y^T = [1\ -1] \tag{3.5}$$

$$f_x = f_y^T = [1\ 0\ -1] \tag{3.6}$$

$$f_x = f_y^T = [1 \ldots 0 \ldots -1] \tag{3.7}$$

It is important to compute the gradient magnitude to eliminate non-edge pixels. Gradient magnitude and direction are computed as follows;

$$|\triangle I| = \sqrt{(f_x * I)^2 + (f_y * I)^2} \tag{3.8}$$

$$\theta(\triangle I) = \arctan\left(\frac{f_y * I}{f_x * I}\right) \tag{3.9}$$

Edge detection is based on thresholding gradient magnitude value of the I image. When the threshold is high , few edge information is captured. With low threshold values, too much detail is present in the result.Several methods like non-maximal suppression are proposed to overcome the problems of this technique. Non-maximum

suppression is often used along with edge detection algorithms. The image is scanned along the image gradient direction, and if pixels are not part of the local maxima they are set to zero. This has the effect of suppressing all image information that is not part of local maxima.

Canny edge detection is a well-known edge detection technique using a Gaussian kernel and non-maximal suppression. Canny and gradient-based edge detection methods give good results on well-defined road marks. However in the case of shadows there are unexpected results as the reader can see in Figure 3.5 and Figure 3.7. In those techniques, thresholds are based on the root mean square (RMS) which is the mean of the magnitude squared image, a value that's roughly proportional to signal to noise ratio (SNR). Threshold of Canny function has been set as 0.2 to eliminate noise in the example figures.

Steerable filters proposed by McCall and Trivedi [15] are also dependent on gradient vectors. The results of steerable filters on the whole ROMA database are very successful [2]. However, their complexity is a drawback; simpler vertical filters or top-hat filters similar successful results with much less complexity[2]. Steerable filters provide the position of lane marks which is a very similar to ridge detection.

Top-hat filter is another type of filter convolved with the image to extract constant width lane marks. The width of lane marks is equalized using IPM or with a linear function which computes lane width according to distance to the bottom line and horizon of the image. Complexity of top-hat filter is less than the steerable filter, however it produces similar results[2].

3.1.2. Ridge Based Methods

Ridge and valley detection techniques have been used in multiple areas like road detection in aerial images, blood vessel detection in retinal images or three-dimensional magnetic resonance images (MRI) and finger print detection. Lopez *et al.* proposed to use ridge property of lane marks as the extraction feature in their work [6]. They have

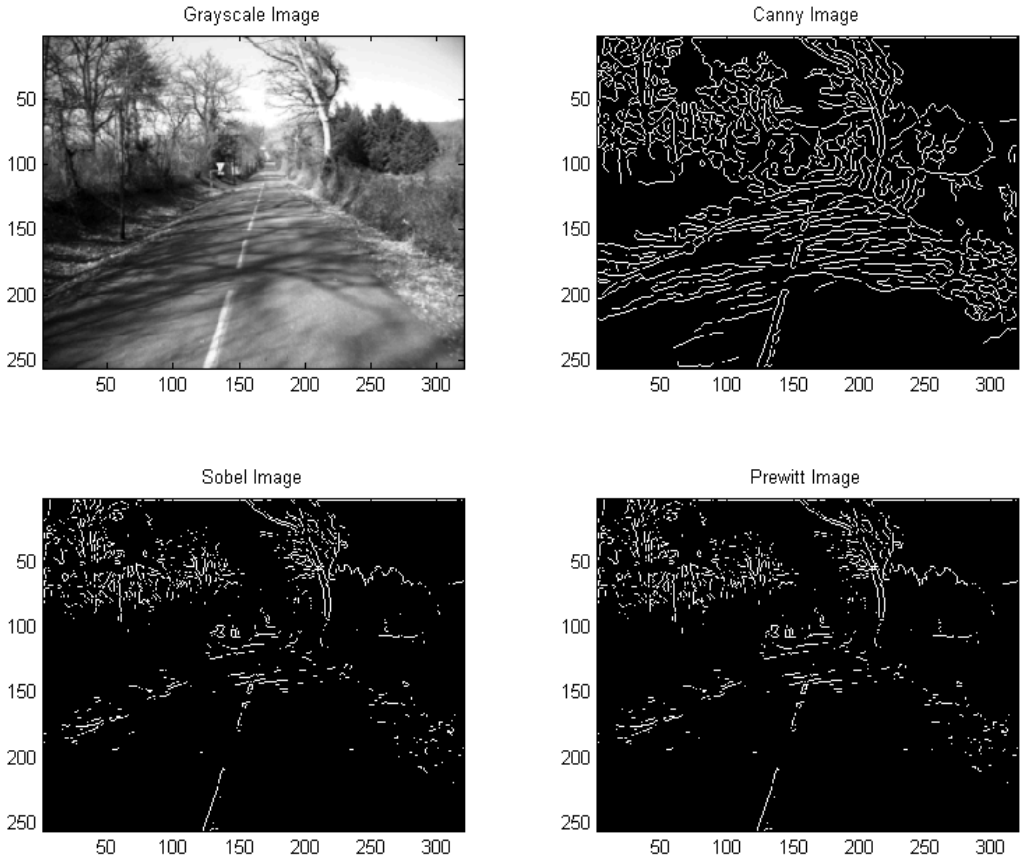

Figure 3.5. Edge detection on an image with shadows

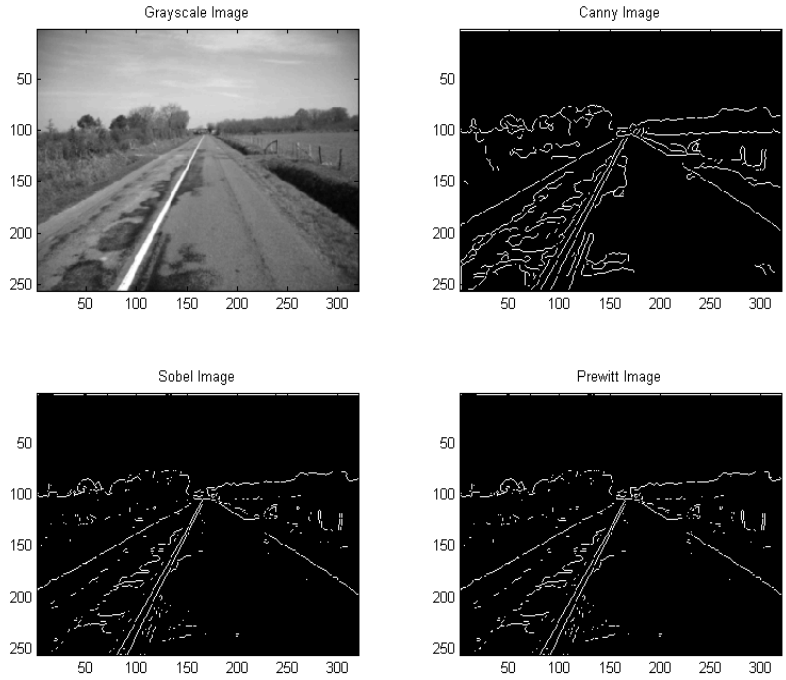

Figure 3.6. Edge detection on an image with tar

defined ridges of a gray scale image as the center lines of elongated, bright structures[32] in the images. In the case of road images, ridge detection picks out the center line of lane markers, which seems more robust than simple gradient vectors and edges.

The main steps of ridge detection is summarized as below [6];

(i). Smooth the image with Gaussian kernel with differentiation scale σ_d

(ii). Compute the gradient vector field $w_{\sigma_d}(\boldsymbol{x})$

(iii). Compute structure tensor field S_{σ_d,σ_i}, with integration scale σ_i

(iv). Compute the eigenvector with highest eigenvalue of S_{σ_d,σ_i} which is $w'_{\sigma_d,\sigma_i}(\boldsymbol{x})$. Then project it on gradient vector field $w_{\sigma_d}(\boldsymbol{x})$ and get the normalized gradient vector field $\tilde{w}_{\sigma_d,\sigma_i}(x)$

(v). Find positive values of divergence (div) of the normalized vector field $\tilde{w}_{\sigma_d,\sigma_i}(x)$ namely ;

$$\tilde{\kappa}_{\sigma_d,\sigma_i}(x) = -div(\tilde{w}_{\sigma_d,\sigma_i}(x)) \tag{3.10}$$

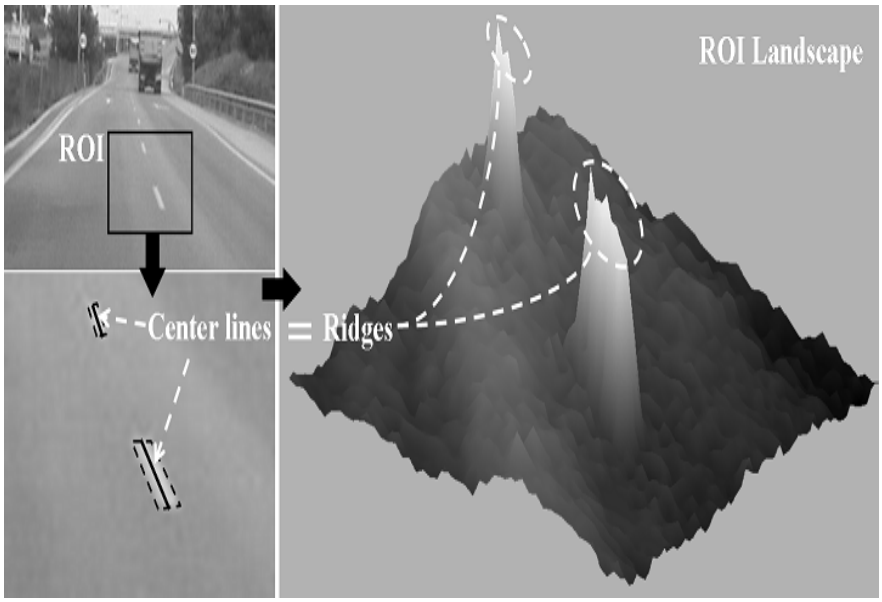

Figure 3.7. Ridge detection of a road image, region of interest (ROI) is the region of lane marks

Ridge based methods also produce successful results on road images with shadows, since the method depends on the orientation, and not on the magnitude of the gradient.

3.1.3. Intensity Based Methods

Color images which have been transformed to gray scale have been widely used in intensity based methods[33], [22], [23].

In RALPH [33] scan line intensity profile representation is generated for each line in the region of interest. The result is compared with the templates generated. The most similar hypothesis is selected to be the representation of the road. The dark-bright-dark transitions are identified as the peaks in the scan line intensity profile. The type of the marker and lighting change affects the method.

Another scan line processing is proposed in [22]. Bright segments over a darker background are searched while the size of the lane width is known a priori. Local thresholding technique is used because intensity values change in the presence of shadows and bright lights. Threshold value depends on the neighbor pixels on both sides

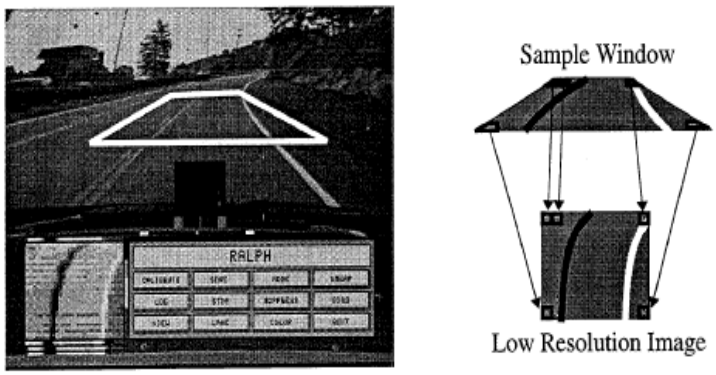

Figure 3.8. RALPH Image Processing Method[33]

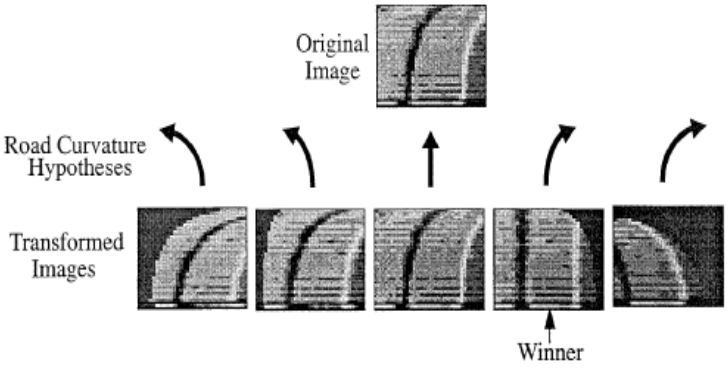

Figure 3.9. RALPH Road curvature solution[33]

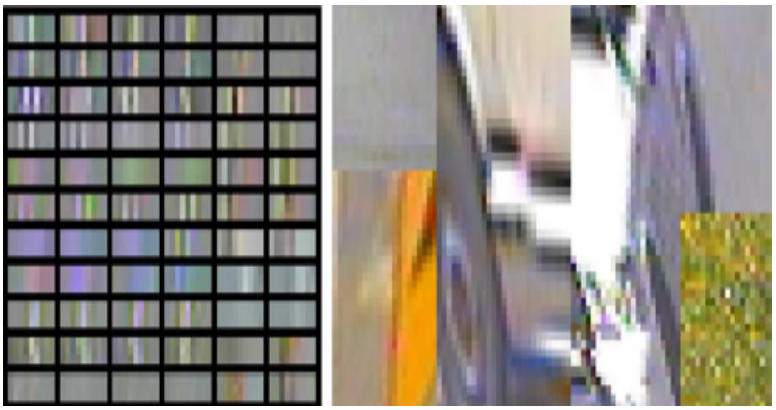

Figure 3.10. Lane and non-lane classified image patches

of the current pixel. Diebolt also proposed to process only the luminance peaks to decrease computation time. This method is robust to shadows and eroded markings. Furthermore, Radon transform has been used in [23] to cover curvature lanes.

3.1.4. Machine Learning Based Methods

Zu Kim proposed to use machine learning techniques to reduce false alarms faced in lane extraction [25]. Artificial neural networks have been applied in various color-based feature extraction methods. Within his work, Kim evaluated the performance of different classifiers. Original road image has been rectified to remove perspective effect using DLT. Then the image is divided into 9x3 windows as reader can see in Figure 3.10. Classifiers are trained with RGB values of 9x3 sub-images, totally 81 features.

3.2. Vehicle-Road Model

Sensor system of an experimental intelligent vehicle includes cameras mounted on the front part of the vehicle (on the roof of the vehicle or on the trunk or behind the rear-view mirror inside the car) facing ahead of the vehicle. Multiple cameras have been used for stereo vision just like in BRAiVE shown in Figure 3.11. The cameras installed at the back of the car are utilized for other purposes, e.g. collision detection, surveillance.

In some of the previous works, roads are generally modeled as parallel straight

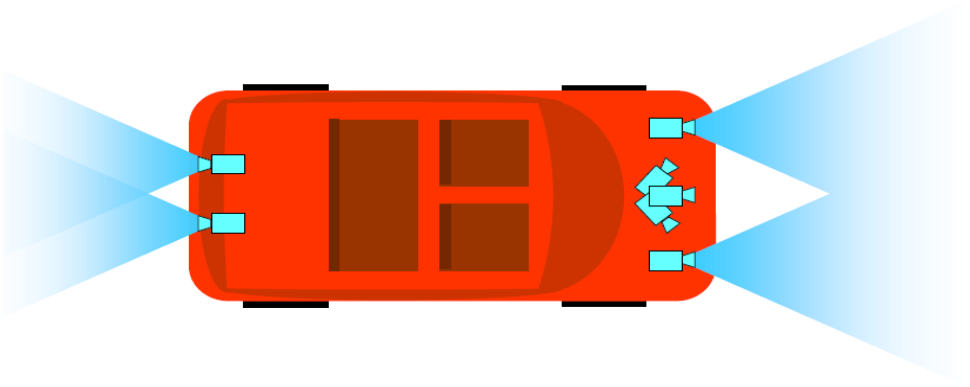

Figure 3.11. Stereo vision in BRAiVE

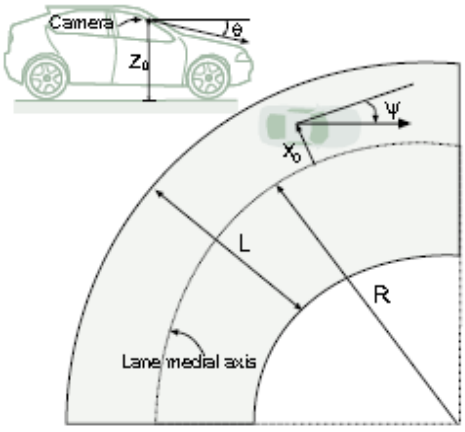

Figure 3.12. Image acquisition geometry

lines after the perspective effect on the image is removed. Since Bertozzi and Broggi introduced inverse perspective mapping(IPM) [10], it has been widely used in lane extraction methods and road models. Direct linear transformation (DLT) is another method, which transforms the original image to a view seen from high in the air (bird's eye view). IPM and DLT methods are described in detail in the following sections. Hough transform is very common to extract lines from the transformed images [34].

In other works, straight segments and circular arcs connected by transition curves are used to model horizontal road geometry[6].Basic assumptions of these approaches about the vehicle and the road are;

(i). Road/lane has constant width
(ii). Road is on a flat plane
(iii). Road/lane has a constant curvature

Under these assumptions, Guiducci has shown that a curved lane marking is projected into the image plane as a branch of a hyperbola with a horizontal asymptote very close to the horizon line [5].

Deformable-templates and likelihood functions have been used to model the lane-marking pixels with model parameters in [26] and [24] in which lane-marking pixels have been modeled as hyperbolas. Zhou et al. have described the meanings of their model as being explicit.

Curved roads have also been modeled as cubic polynomials [25]. Lane-marking pixels are grouped into uniform cubic-spline curves of two or four control points. Cubic-splines curves are fitted with RANSAC algorithm in [25].

3.3. Lane Tracking

Tracking the parameters of the vehicle pose and the road model is a challenging task. Early models have focused on steering response to a given road image as input.

Control functions of ALVINN (Autonomous Land Vehicle in a Neural Net) are based on this method. However, the majority of lane tracking systems include an explicit road model which enables the control system to produce complex steering response.

Within the PROMETHEUS project, the team at the Universit at der Bundeswher led by Professor Dickmanns has proposed a successful approach to lane localization and tracking problem. Dynamical model of the vehicle is very detailed, and they use extended Kalman filter to estimate vehicle and road state parameters. They have proposed the 4-D approach which is a combination of a bottom-up and top-down method for road and lane recognition. Bottom-up estimation is an independent process that determines the road structure using edge features while the top-down prediction and validation of road models. Using extended Kalman filter, model of the world in space (3D) and in time (1D) are incorporated.

Strong temporal coherence which enforced with the 4D-approach has made Dickmanns algorithm successful in many conditions. As Apostoloff has stated in his thesis[14];

"The success of Dickmanns algorithm can largely be attributed to the strong dynamical models for vehicle motion used in conjunction with the recursive 4D approach to machine vision. While the edge feature detectors that were used were novel and powerful for their day, they were nonetheless based on simple edge extraction which can still be fooled by erroneous edges. It was the strong temporal coherence enforced with the 4D-approach that allowed them to succeed where others had failed. This directed search for edge features reduced the complexity of a potentially expensive image processing algorithm and was particularly useful for structured man-made environments. However, the major limitation in their approach was that it struggled with variations in the driving environment (i.e. construction zones, dramatic lightning changes, poor or no lane markings, shadows across the road, etc.) since edge-based feature detection was the primary means of lane extraction. While the extended Kalman filter enforced temporal consistency, it is inherently a unimodal technique that is prone to failure if the posterior distribution used for tracking is non-Gaussian. By restricting the visual

search space using predictions from the tracking algorithm, they overcame many of the problems associated with multimodal posterior distributions, however this was not sufficient to deal with the uncertainty of semi-structured roads that contain poor lane markings or inconsistent structure."

It can be concluded that, the importance of the lane feature extraction is very dominant over the tracking algorithm in the challenging conditions. Temporal coherence is used whenever the extraction does fail in those conditions.

3.4. Direct Linear Transformation (DLT)

Direct Linear Transformation (DLT) algorithm [4] is a well-known method to find the camera projection matrix. In the field of lane detection this method is used to remove the perspective effect on the image. The road is viewed from high in the air (bird's eye view). A homography matrix is formed, which converts the image coordinates to the world coordinates in which values on Z axis is equal to zero. This requires the assumption that the road is flat. As a result, X and Y axis of the world coordinates are rectified to new image by scaling factor. When we assume the road is flat, we can apply plane homography in which a point (x, y) on the rectified image corresponds to the point (u, v) in the original image and H is a homography matrix in the DLT equation 3.11.

$$\begin{pmatrix} \lambda x \\ \lambda y \\ \lambda \end{pmatrix} = H \begin{pmatrix} u \\ v \\ 1 \end{pmatrix} \tag{3.11}$$

At least four reference points are necessary to solve the homography matrix. Details on the plane homography are explained in [4] as follows;

Figure 3.13. Original Image

Given $n \geq 4$ 2D to 2D point correspondences $\{x_i \leftrightarrow x_i^{'}\}$, determine the 2D homography matrix H such that $x_i^{'} = Hx_i$.

Follow the below algorithm ;

(i). For each correspondences $x_i \leftrightarrow x_i^{'}$ compute the matrix $\boldsymbol{A_i}$ which satisfies $\boldsymbol{A_i h} = 0$.

(ii). Assemble the n 2×9 matrices $\boldsymbol{A_i}$ into a single $2n \times 9$ matrix $\boldsymbol{A}$.

(iii). Obtain the singular value decomposition (SVD) of $\boldsymbol{A}$. The unit singular vector corresponding to the smallest singular value is the solution $\boldsymbol{h}$. Specifically, if $\boldsymbol{A} = UDV^T$ with D diagonal with positive entries, arranged in descending order down the diagonal, then $\boldsymbol{h}$ is the last column of V.

(iv). The matrix H is determined from $\boldsymbol{h}$.

The effect of rectifying on road images with DLT can be seen in the following images. Borders of the lane marks are blurred, and edges are not sharp. However, the widths of the lanes are equal and the lanes on the right and left side of the vehicle are parallel to each other.

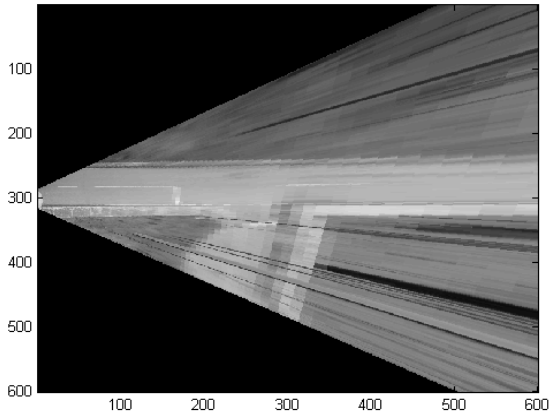

Figure 3.14. Rectified Image

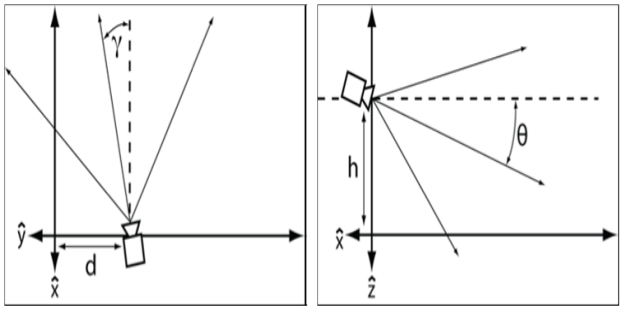

Figure 3.15. Camera Top View and Side View

3.5. Inverse Perspective Mapping (IPM)

"The Inverse Perspective Mapping (IPM) geometrical transform belongs to the resampling filters family: the initial image is non-homogeneously resampled, in order to produce a new image that represents the same scene as acquired from a different position."[35][10]. There are various lane detection methods utilizing IPM in order to remove perspective effect from the image.

The IPM method [10] transforms between the 3D Euclidean space and 2D Euclidean space defined as follows;

$W = (x, y, z) \in E^3$ represents the 3D world space (world coordinate system) with coordinates in meters

$I = (u, v) \in E^2$ represents the 2D image space (image-coordinate system) with coordinates of each pixel

The image acquired by the camera is represented in I space while the remapped image belongs to the $z = 0$ plane of W space. To remap the image, the following parameters from 3.15 must be known: $C = (l, d, h) \in W$ camera position in world coordinates, γ camera yaw, θ camera pitch, α angular aperture, $n \times n$ camera resolution. The transformation from world coordinates to image coordinates in[10] is $W \rightarrow I$

$$u(x, y, 0) = \frac{\arctan\left(h \sin\left[\arctan(\frac{y-d}{x-l})\right]\right) - (\theta - \alpha)}{\frac{2\alpha}{n-1}} \tag{3.12}$$

$$v(x, y, 0) = \frac{\arctan\left(\frac{y-d}{x-l}\right) - (\gamma - \alpha)}{\frac{2\alpha}{n-1}} \tag{3.13}$$

The transformation from image coordinates to world coordinates in[10] is $I \rightarrow W$

$$x(u, v) = h \cot\left[(\theta - \alpha) + u\frac{2\alpha}{n-1}\right] \sin\left[(\gamma - \alpha) + v\frac{2\alpha}{n-1}\right] + l \tag{3.14}$$

$$y(u, v) = h \cot\left[(\theta - \alpha) + u\frac{2\alpha}{n-1}\right] cos\left[(\gamma - \alpha) + v\frac{2\alpha}{n-1}\right] + d \tag{3.15}$$

As you can see, IPM transformation deforms straight lines. The equations of Broggi and Bertozzi **??** remove the perspective effect of the camera, however straight horizontal lines become curved lines and distance to horizontal lines is not right . This is a problem that has been solved by Johnson and Hamburger in their project [36]. The new transformation from image coordinates to world coordinates $I \rightarrow W$ is defined as follows;

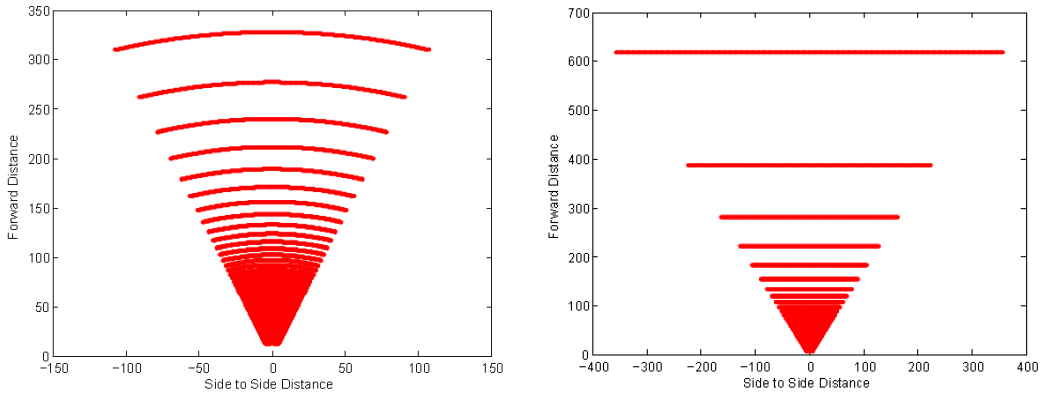

(a) Broggi and Bertozzi's IPM transformation (b) Eric Johnson's IPM transformation

Figure 3.16. IPM transformation

α_u horizontal angular aperture α_v vertical angular aperture

$$R = \left(1 - \frac{2(u-1)}{n-1}\right) \tan(\alpha_v) \tag{3.16}$$

$$x(u) = h\frac{1 + R\tan(\theta)}{tan(\theta - R)} \; \forall v \in [1, n] \tag{3.17}$$

$$y(u,v) = h\frac{\left(1 - \frac{2(c-1)}{n-1}\right)\tan(\alpha_u)}{\sin(\theta) - R\cos(\theta)} \tag{3.18}$$

The difference between IPM with Bertozzi,Broggi[10] and with [36] equations can be seen in the Figure 3.16. As a result the updated version of IPM is more accurate than the original one. Two sample image is transformed with the updated equations in Figure 3.17 and in Figure 3.18.

IPM is a very well know transformation technique to remove perspective effective. However it has been modeled on flat surface and gives inaccurate results non-flat roads. We have considered other linear method to remove perspective effect to reduce complexity.

(a) Original image

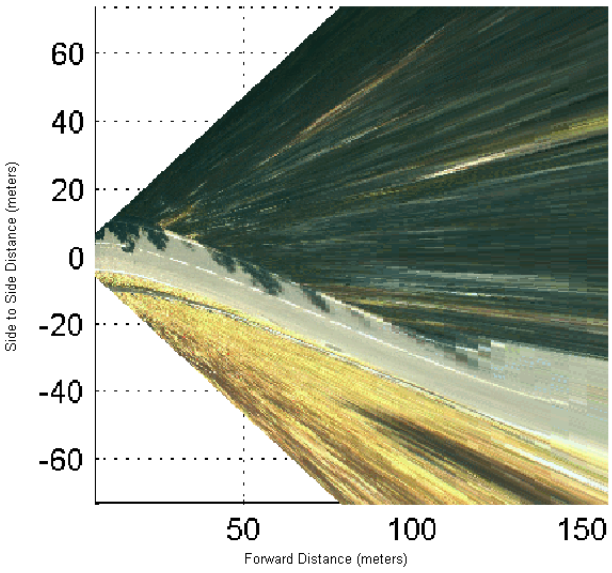

(b) Transformed image

Figure 3.17. Updated IPM transformation on ROMA image

(a) Original image

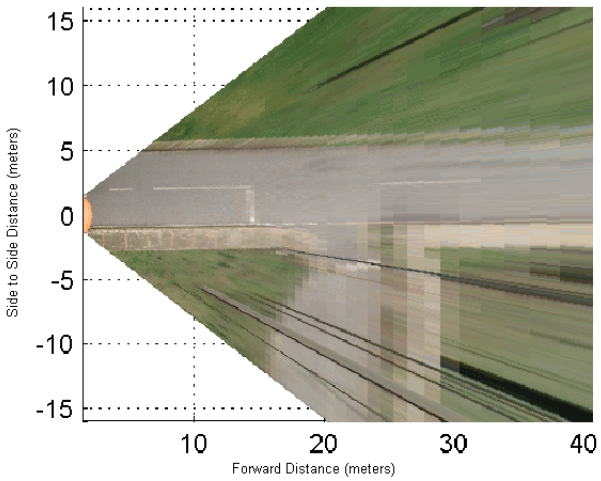

(b) Transformed image

Figure 3.18. Updated IPM transformation on a sample image

3.6. RANSAC

The RANdom Sample And Consensus (RANSAC) algorithm was first introduced by Fischler and Bolles [3] in 1981 as a method to estimate the parameters of a certain model starting from a set of data contaminated by large amounts of outliers. The percentage of outliers which can be handled by RANSAC can be larger than 50% of the entire data set. Such a percentage, know also as the breakdown point, is commonly assumed to be the practical limit for many other commonly used techniques for parameter estimation (such as all the least squares flavors or robust techniques like M-estimators and least median of squares.[37]

Despite many modifications, the RANSAC algorithm is essentially composed of two steps that are repeated in an iterative fashion (hypothesize-and-test framework)[37]:

(i). Hypothesize : First minimal sample sets are randomly selected from the input data set and the model parameters are computed using only the elements of these sample sets. The cardinality of the sets is the smallest sufficient to determine the model parameters (in contrast to opposed to other approaches, such as least squares, where the parameters are estimated using all the data available, possibly with appropriate weights).

(ii). Test : In the second step RANSAC checks which elements of the entire data set are consistent with the model instantiated with the parameters estimated in the first step. The set of such elements is called consensus set (CS). RANSAC terminates when the probability of finding a better ranked CS drops below a certain threshold. In the original formulation the ranking of the CS was its cardinality (i.e. CSs that contain more elements are ranked better than CSs that contain fewer elements).

4. PROPOSED LANE DETECTION SYSTEM

4.1. Lane Extraction

Road scenes with strong shadows cause unexpected results in edge-based extractors. On the other hand, local intensity comparison will be successful to detect lanes with brighter colors painted on the dark road surface under shadow. One of the strong techniques is the symmetrical local threshold which is introduced in [22] [23]. The version in [2] requires an acceptability width range with minimum and maximum values $[L_m, L_M]$ for selecting horizontal segments as road marking elements. These ranges are constant if the perspective effect is removed from the image with a transformation method like IPM [10]. Another method is computing range values for each line assuming that lanes are at their maximum width at the bottom line of the image and decreases linearly as moving to the horizon. The feature extraction method in our work is similar to symmetrical local threshold. In this technique, on each line under the horizon, each point is compared with the intensity average of left and right neighbors within a window defined by maximum lane width. The pixel having intensity higher than left and right neighbor pixels with given threshold is selected to be a candidate lane pixel [2] . Local threshold method which is implemented in this theses is powerful to detect eroded lane marks and road borders. We have summarized the algorithm flowchart in figure 4.1.

Let I be the image to be processed and W be the new image containing the lane candidate pixels and (u, v) denote the pixel coordinates

$$W(u,v) = \begin{cases} 1 & if\ I(u,v) > mean(I(u,p_i)) + T \quad and \quad I(u,v) > mean(I(u,p_j)) + T \\ 0 & otherwise \end{cases} \tag{4.1}$$

$where\ p_i = [v-w, v]\,, p_j = [v, v+w]\,, w \in [L_m, L_M].$

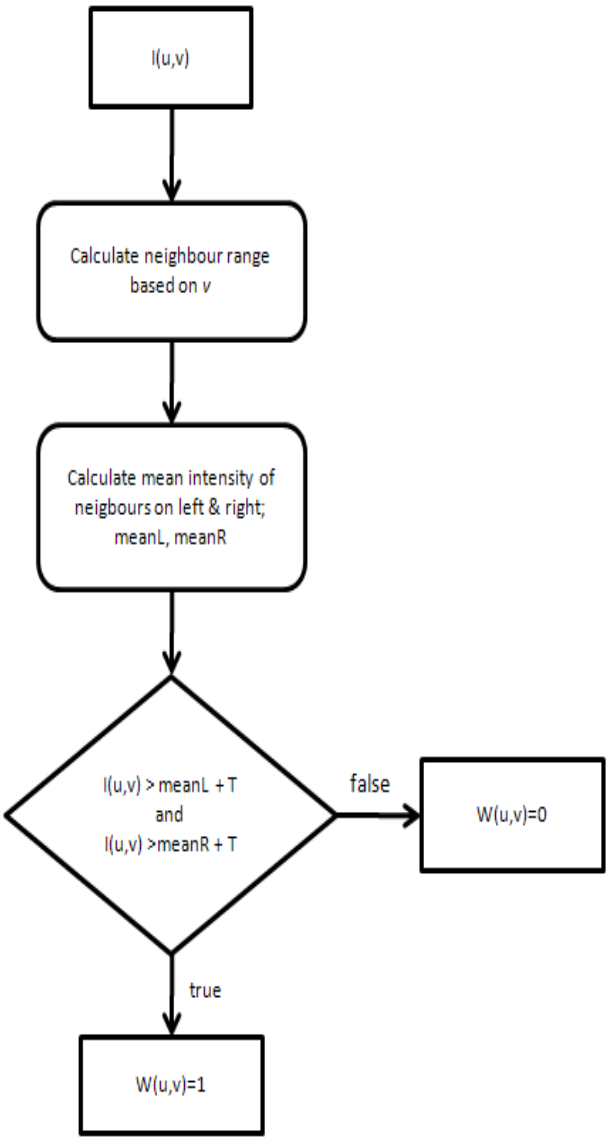

Figure 4.1. Symmetrical Local Threshold

We have preferred to process gray level images to reduce complexity. Colored images are converted to grayscale with a weight vector [0.6, 0.3, 0.1] emphasizing yellow lane marking. Different weight values are proposed in [19]. However, we also try to eliminate the green color. The result of the first extraction phase is processed to separate road lane pixels from the false detections. RANSAC algorithm fits a line for lanes or road sides on the left and right of the camera. The error and variance parameters in RANSAC are important for detection, especially in shadow regions. Since line patterns in the image have smaller variance than bright regions caused by shadows of the trees. Sample images are presented in 5.1 with several types of road scenes, which have strong tree shadows, eroded road markings and roads with high curvature. Extraction algorithm output is plotted with blue marks on the original image. Left lane is colored with red and right lane is colored with green. Within the previous works in the literature, evaluation of lane detection techniques is generally presented on the original image, and those images are not part of a reference database. As we mentioned earlier in their recent study Veit et al. proposed performance metrics [2] for systematic evaluateion of lane feature extraction algorithms. They have built the reference database ROad MArkings (ROMA) containing over 100 images of natural road scenes available in their website [38] and proposed Receiver Operating Characteristic (ROC) and Dice Similarity Coefficient (DSC) metrics [2]. ROC and DSC curves of symmetrical local threshold on this database of 110 images are presented in Fig. 3. ROC curves present the ratio of True Positive Rate (TPR) over False Positive Rate (FPR) of the algorithm output given a range of threshold values. Threshold value should be an input parameter to the algorithm which is able to control the algorithm output. This is a well-known metric in image processing literature and used for representing algorithm performance. Lager area under a ROC curve indicates better performance. The larger area under the blue ROC curve shows that the extraction on normal images is better than the extraction performance on images with high curvature and adverse lighting conditions, as expected. DSC metric is preferred to evaluate the segmentation of small structures in medical image analysis [2] . Since the proportion of lane pixels in the image is small, DSC is also used in evaluation of lane feature extraction algorithms [2] . The maximum value in DSC curve corresponds to the optimal threshold value and maximum dice value (Dice Max) of the algorithm. The DSC measures of the algorithm

Table 4.1. DSC Measures

Condition	Dice Max	TPR	Threshold
Adverse light	0.6011	0.5420	16
High curvature	0.6068	0.5372	15
Normal	0.7974	0.7297	21

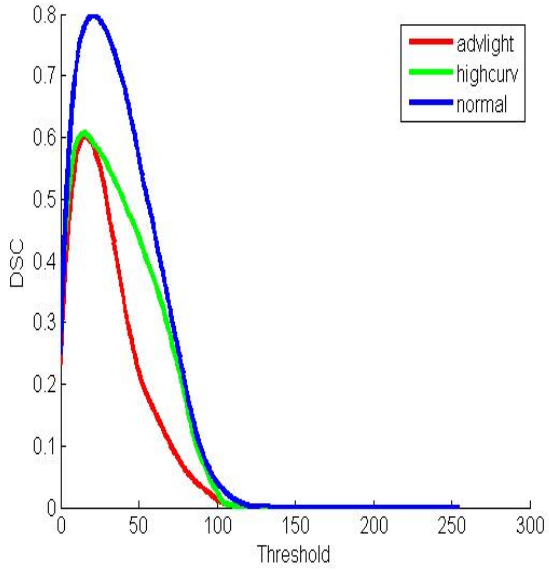

Figure 4.2. DSC curve of lane extraction on database

are listed in Table 1. Threshold value for this algorithm is gray scale intensity that is the difference limit between a pixel with its neighbors. The width of the peak in the DSC curve presents the sensitivity of the algorithm with respect to the threshold tuning. The algorithm is more sensitive to threshold tuning in case of images with high curvatures. The result of the lane feature extraction still contains false positive lane detection pixels. In order to eliminate outliers, inliers fitting to a line model are selected with RANSAC. Variance parameter of the algorithm can be reduced for accuracy. However eroded line marks are easily detected with larger variance. Left and right region of the image coordinate system are separated by the center horizontal axis. In the case of high curvatures, curvature value can be used to identify the separating axis between left and right regions with a border specified with a gradient value of central axis. In comparison with

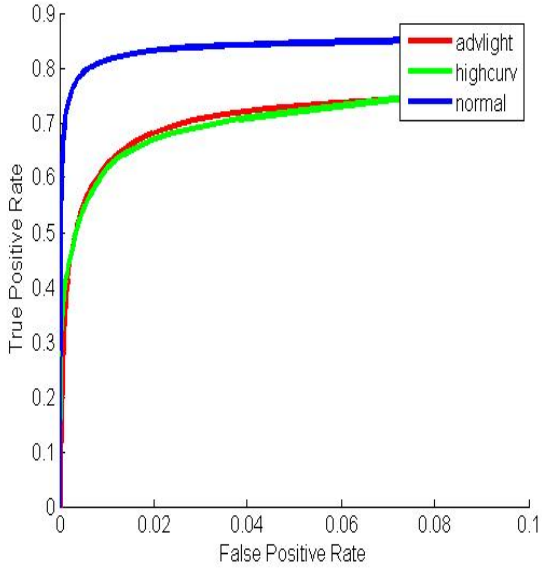

Figure 4.3. ROC curves of lane extraction on database

Generally, center-lane pixels are dominant and there are few lane marks on the road border mark on suburban roads. However, the algorithm still works on such conditions and detects the center lane as the left lane and road border as the right lane. Estimation of lanes on both sides is very effective in the calculation of road width and vehicle lateral position as we will see in the next section.

4.2. Lane Model - Pair of Hyperbolas

Geometric models of the road lane are crucial for lane detection applications. Road models based on parallel lines seem to be sufficient in highway applications. However, in freeways and urban traffic it is required to have a model handling the curvature. In our model, we use parallel hyperbola pairs to represent the left the left and right lanes. This model is proposed in [5] with the assumptions in [18]. The model is very efficient in order to derive road and vehicle parameters to control an autonomous vehicle. The camera and image coordinates are visualized in figure 4.2 with the lane model. The camera is x_c located meters from the center of the lane and at height H above the ground. Height of the camera is constant. Vehicle direction and camera pitch angle are represented with θ (yaw angle) and ϕ (pitch angle) respectively. The camera calibration parameters E_u and E_v are the focal lengths in pixel/meter along

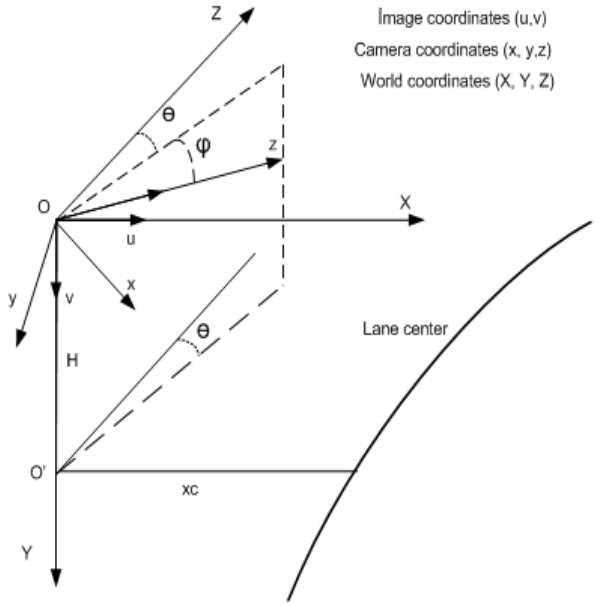

Figure 4.4. Lane geometry with world,camera and image coordinates

horizontal and vertical camera axes. The following equation relates right and left lane pixel coordinates (u, v) with road and camera parameters [5];

$$u_L = E_u \left(\frac{(v - E_v\varphi)}{HE_v} \left(x_c - \frac{L}{2} \right) - \frac{E_v H C_0}{2(v - E_v\varphi)} - \theta \right)$$

$$u_R = E_u \left(\frac{(v - E_v\varphi)}{HE_v} \left(x_c + \frac{L}{2} \right) - \frac{E_v H C_0}{2(v - E_v\varphi)} - \theta \right) \tag{4.2}$$

Parallel hyperbolas are introduced in [6] with the parameters x_c and L which are the distance from the center of the lane and lane width respectively. The parameters E_u, E_v , H and ϕ can be estimated through calibration.

The linear equation proposed in [6],[32] is defined by the set of ridgel coordinates of lane marks on the left and right side. It is just an expression of 4.2 in a linear form with pixels for both left and right lanes. Our system does not use ridgeness and

classifies left and right lanes in the lane selection phase. So that we can still use the linear equation while ϕ is known;

The set of linear equations: where $\boldsymbol{a} = (a_1, a_2, a_3, a_4)^T$, and the set of left lane pixels are $(\boldsymbol{u_L}, \boldsymbol{v_L}) = (\{u_{L,i}\}, \{v_{L,i}\}) \qquad \forall i = 1, \ldots, N_L$ and the set of right lane pixels are $(\boldsymbol{u_R}, \boldsymbol{v_R}) = (\{u_{R,i}\}, \{v_{R,i}\}) \qquad \forall i = 1, \ldots, N_R$, these pixels satifies the linear equation below which is an expression of model in equation 4.2;

$$\begin{pmatrix} 1 & (E_v\varphi - \boldsymbol{v_L}) & (\boldsymbol{v_L} - E_v\varphi) & \frac{1}{\boldsymbol{v_L} - E_v} \\ 1 & (\boldsymbol{v_R} - E_v\varphi) & (\boldsymbol{v_R} - E_v\varphi) & \frac{1}{\boldsymbol{v_R} - E_v} \end{pmatrix} \boldsymbol{a} = \begin{pmatrix} \boldsymbol{u_L} \\ \boldsymbol{u_R} \end{pmatrix} \tag{4.3}$$

Lane model parameters are related with the vector a as follows;

$$\theta = -\frac{a_1}{E_u}, \;\; L = -\frac{2HE_v a_2}{E_u}, \;\; C_0 = -\frac{2a_4}{HE_v E_u}, \;\; x_c = -\frac{HE_v a_3}{E_u} \tag{4.4}$$

In order to solve four unknowns in the vector, 4 lane pixels are necessary. And at least one of them should be on a different side. Generally, we have more than 4 lane pixels and select optimal lane pixels with RANSAC. This is a similar technique proposed in [6]. However, we are using different error function, and we don't use any ridgeness information. Still ridge-based method in [6] is not working on images without lane mark on the left side. Within our method using brighter pixels as lane candidates enable our system to estimate left lane.

4.3. Model Fit with RANSAC

RANSAC has been applied to various computer vision problems. We have applied RANSAC as follows; two main regions are defined, one for the bottom part of the image, one for the region close to the horizon. Four lane pixels are selected from each of those regions, and a parallel hyperbola model is generated. Since the error function is defined as a distance measure, distance of the other lane pixels to the hyperbola is

computed and the ones less than the error tolerance are selected to form a consensus set. If the number of pixels in the consensus set is higher than the consensus threshold, the lane model is computed again with all the points in the consensus set to form the best fit. We assume that the closest point on the hyperbola to a point is the corresponding pixel satisfying the equation with the same vertical image coordinate of that point. This error function is simple and easy to implement while producing satisfying results. To accomplish an optimal fit, it is important that the data contains a reasonable percentage of inliers. Our extraction method generally detects most of the lane pixels. Still false positive detections or outliers should calculate the vehicle lateral position, road curvature and lane width parameters accurately.

5. Results and Performance Evaluation

5.1. Results

Results of lane detection in the literature are often presented in the form of several frames on which the correspondence of the detected lane lines with the real lane markings are plotted on the original image. Here is the a similar result of our technique. Following sample images are selected from ROMA database.

The algorithm successfully detects the road border when there is no lane mark and fits the hyperbola-pair. It is clearly observed in sample images row 1-2 in images listed in figure 5.1. The proposed method gives promising results on images with strong shadows (row 1, 3). Shadows create clutter with the lane extraction method since many brighter regions are detected as lane pixel candidates. True lane pixels form a regular shape; however, shadow pixels generally form an irregular shape. Lane selection based on RANSAC line model fits a regular model and selects the lanes successfully. Various road textures caused by tar like the image in row 2 do not affect the lane selection, since they do not appear to be lane pixel in feature extraction phase. Curved roads with small curvature value (row 4) are also successfully processed with this method. Some of the results on the sample images of ROMA are presented in figure 5.1. As the reader can see eroded lanes or lane under shadow are detected successfully.

Another evaluation method proposed in the literature is to compare the computed road and vehicle parameters with the ground truth information of synthetic images generated with a simulator [32]. Estimating the lane and vehicle parameters with hyperbola model fitting with RANSAC produces promising results on synthetic images. However, any false lane selection directly affects the lane model as it can be observed in figure 5.1.

When the center road lane is not dominant, algorithm selects far left lane and the estimated width of lane is doubled as a result. Curvature value is very small,

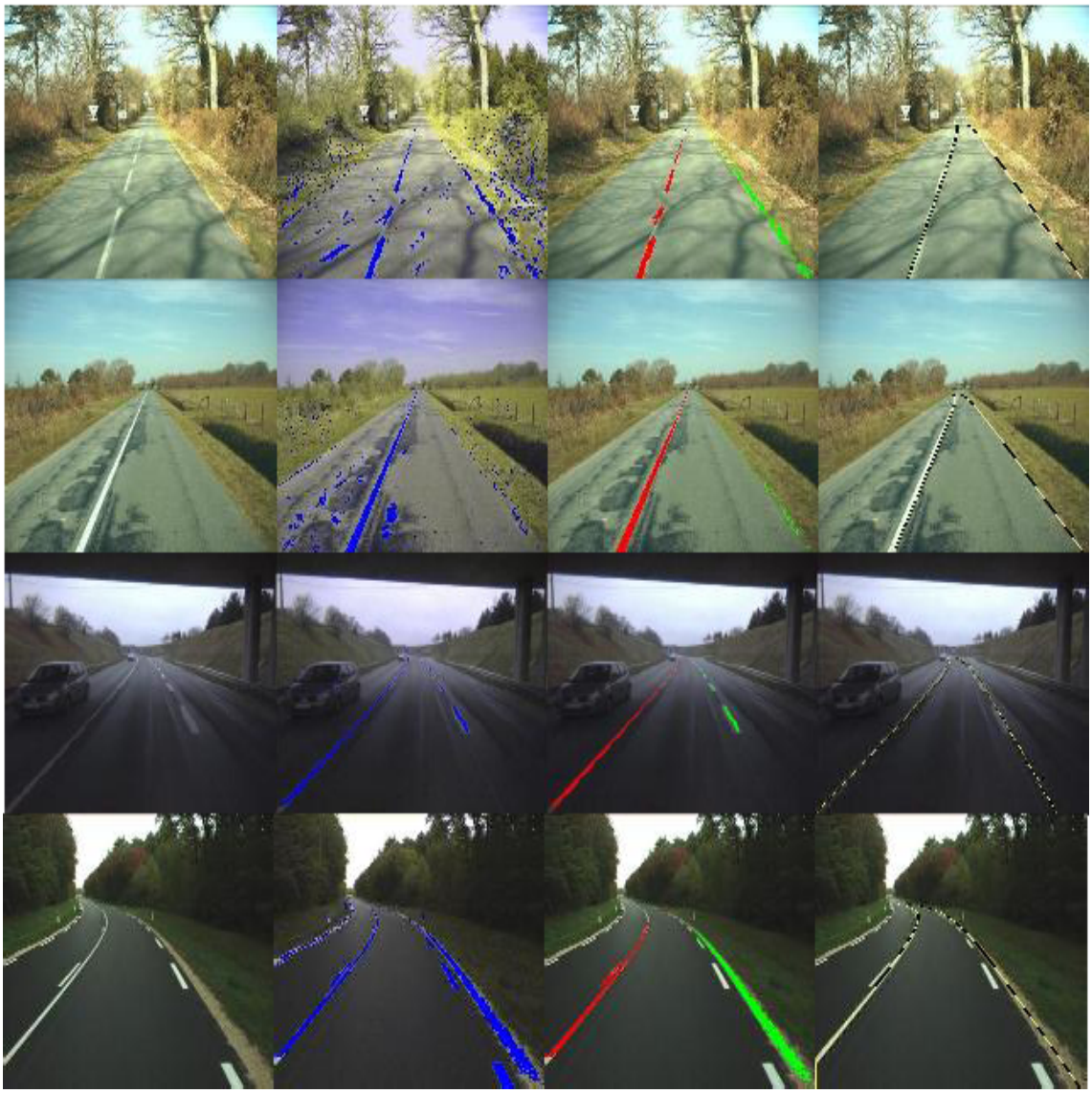

Figure 5.1. Intermediate Results on sample images of ROMA; first column original image, second coloumn feature extraction, third left-right lane selection, fourth hyperbola-pairs

Figure 5.2. Results on sample images of ROMA

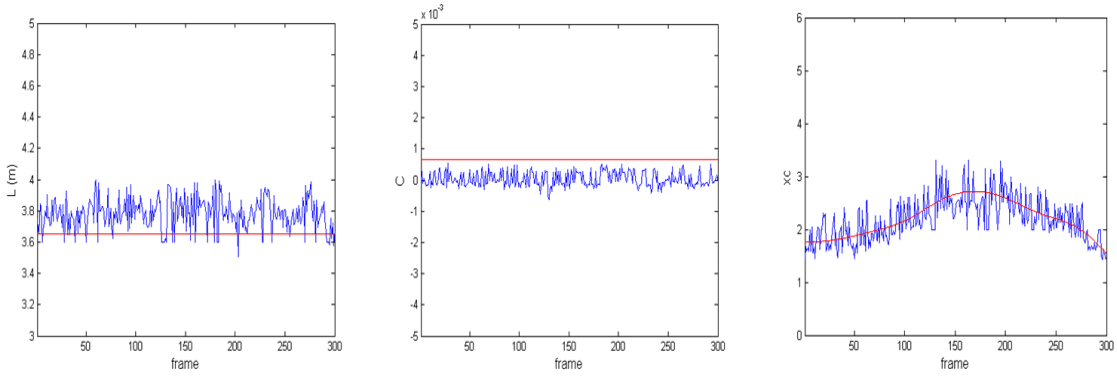

Figure 5.3. Estimated Lane and Vehicle Parameters, L is Lane width, C is road curvature and x_c is lateral position

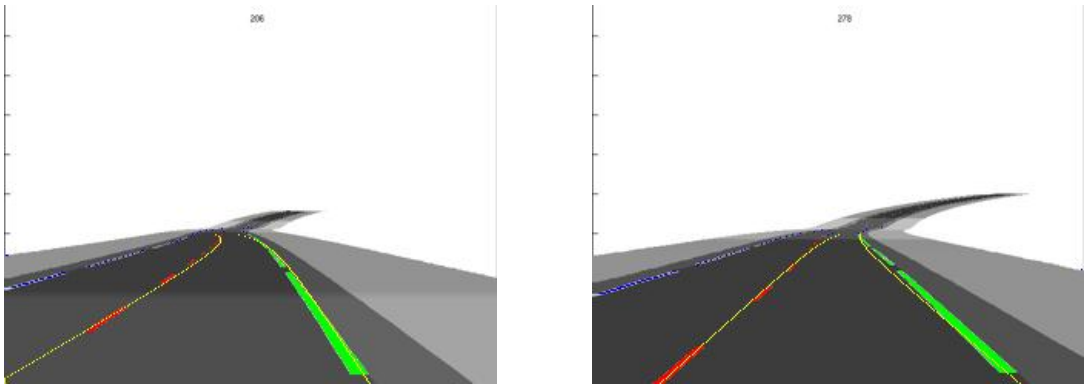

Figure 5.4. Samples from Synthetic Image Sequence

but saturating on the sample sequence. Lateral position estimation is closely related with lane width. Lateral position is estimated with small errors if the selection phase provides true left and right lane pixels. Pitch value is assumed to be constant, although it changes as the road has bumps and holes. The method should be extended to deal with non-planar roads and with very high curvatures. Pitch value can be estimated for non-planar roads by using the data from the previous frames. On the other hand, yaw, pitch and roll values are measured within sensors in an autonomous vehicle. Measured pitch value will be much more efficient if this lane detection system is integrated in an intelligent vehicle. In figure 5.4 reader can see the left and right lane detection with hyperbola-pair on the images numbered 206 and 278 in the synthetic image sequence.

The error rates in 300 images in the sequence are as follows ;

Table 5.1. Error rates on synthetic images

Parameter	Standard deviation	RMS	Absolute Mean Error
x_c (lateral distance)	29.3131 cm	29.3675 cm	25.2329 cm
C (curvature)	2.3367e-004	6.6005e-004	6.1745e-004
L (Lane width)	10.0541 cm	16.5698 cm	14.3092

5.2. Conclusions

The lane detection system that we have proposed produce promising results on images with strong shadows, many extraneous lines and eroded markings. Using the symmetrical local threshold with a selection of lane pixels based on RANSAC line model within a flexible variance forms a reliable set. This set increases the accuracy of calculation of the solution of the linear system formed with lane pixels to estimate road and vehicle parameters in challenging conditions like strong shadows and eroded markings.

The system also fits a hyperbola-pair, even if there is no lane mark on the left side of the road. The right and left lane selection is crucial for curve estimation.

Proposed lane detection can be merged with a tracking system which will enable to decrease the search space for extraction and selection. Estimating a separating line between lanes with the help of previous frames is a part of lane tracking algorithm. As a conclusion the proposed lane detection system is robust to road and lighting conditions and can be easily integrated to an perception system of an unmanned vehicle.

REFERENCES

1. U. Nations, "Decade of Action for Road Safety 2011-2020," 2011.

2. T. Veit, J.-P. Tarel, P. Nicolle, and P. Charbonnier, "Evaluation of Road Marking Feature Extraction," *2008 11th International IEEE Conference on Intelligent Transportation Systems*, pp. 174–181, Oct. 2008.

3. M. A. Fischler and R. C. Bolles, "Random Sample Consensus:Paradigm for Model Fitting with Applications to Image Analysis and Automated Cartography," *Communications of the ACM*, vol. 24, no. 6, 1981.

4. R. Hartley and A. Zisserman, *Multiple view geometry in computer vision*. Cambridge Univ Pr, 2003.

5. A. Guiducci, "Parametric Model of the Perspective Projection of a Road with Applications to Lane Keeping and 3D Road Reconstruction," *Computer Vision and Image Understanding*, vol. 73, pp. 414–427, Mar. 1999.

6. A. Lopez, C. Canero, J. Serrat, J. Saludes, F. Lumbreras, and T. Graf, "Detection of lane markings based on ridgeness and RANSAC," in *Proceedings. 2005 IEEE Intelligent Transportation Systems, 2005.*, pp. 733–738, Ieee.

7. L. Li and F.-Y. Wang, *Advanced Motion Control and Sensing for Intelligent Vehicles*. No. Iv, Springer Science+Business Media, LLC, May 2007.

8. M. Bertozzi, "Vision-based intelligent vehicles: State of the art and perspectives," *Robotics and Autonomous Systems*, vol. 32, pp. 1–16, July 2000.

9. E. D. Dickmanns, "Computer Vision and Highway Automation," *Vehicle System Dynamics*, vol. 31, pp. 325–343, June 1999.

10. M. Bertozzi, A. Broggi, and A. Fascioli, "Stereo Inverse Perspective Mapping :

Theory and Applications," *Image and Vision Computing Journal*, vol. 8, no. 16, pp. 585–590, 1998.

11. S. R. Team, J. Levinson, A. Petrovskaya, and G. Hoffmann, "Stanford s Robotic Vehicle Junior : Interim Report," 2007.

12. G. Motors and A. Continental, "Tartan Racing: A Multi-Modal Approach to the DARPA Urban Challenge," *Defense*, 2007.

13. T. Lead and T. Lead, "Development of the SciAutonics / Auburn Engineering Autonomous Car for the Urban Challenge Prepared for : DARPA Urban Challenge Prepared by : SciAutonics , LLC and Auburn University College of Engineering Submission Date :," *Mechanical Engineering*, no. 805, 2007.

14. N. Apostoloff, "Vision based lane tracking using multiple cues and particle filtering," *PhD thesis, Department of Systems Engineering, Research School of Information Science and Engineering, Australian National University*, 2005.

15. J. McCall and M. Trivedi, "Video-based lane estimation and tracking for driver assistance: survey, system, and evaluation," *IEEE Transactions on Intelligent Transportation Systems*, vol. 7, no. 1, pp. 20–37, 2006.

16. J. Crisman and C. Thorpe, "SCARF: a color vision system that tracks roads and intersections," *IEEE Transactions on Robotics and*, 1993.

17. M. Sotelo, F. Rodriguez, and L. Magdalena, "VIRTUOUS: Vision-Based Road Transportation for Unmanned Operation on Urban-Like Scenarios," *IEEE Transactions on Intelligent Transportation Systems*, vol. 5, pp. 69–83, June 2004.

18. E. Dickmanns and B. Mysliwetz, "Recursive 3-D road and relative ego-state recognition," *IEEE Transactions on pattern analysis and machine intelligence*, vol. 14, no. 2, pp. 199–213, 1992.

19. C. Kreucher, S. Lakshmanan, and K. Kluge, "A Driver Warning System Based on

the LOIS Lane Detection Algorithm," *Artificial Intelligence*.

20. D. Aubert, K. Kluge, and C. Thorpe, "Autonomous navigation of structured city roads," *in SPIE Mobile Robots*, 1990.

21. M. Bertozzi, S. Member, A. Broggi, and A. Member, "GOLD : A Parallel Real-Time Stereo Vision System for Generic Obstacle and Lane Detection," *IEEE Transactions on Image Processing*, vol. 7, no. 1, pp. 62–81, 1998.

22. F. Diebolt, "Road Markings Recognition," *International Conference on Image Processing*, vol. 2, pp. 669–672, 1996.

23. P. Charbonnier, F. Diebolt, Y. Guillard, and F. Peyret, "Road markings recognition using image processing," in *IEEE Conference on Intelligent Transportation System, 1997. ITSC'97.*, pp. 912–917, 1997.

24. Y. Zhou, R. Xu, X. Hu, and Q. Ye, "A robust lane detection and tracking method based on computer vision," *Measurement Science and Technology*, vol. 17, no. 4, pp. 736–745, 2006.

25. Z. Kim, "Robust lane detection and tracking in challenging scenarios," *IEEE Transactions on Intelligent Transportation Systems*, vol. 9, no. 1, pp. 16–26, 2008.

26. K. Kluge and S. Lakshmanan, "A deformable template approach to lane detection," *in Proc. IEEE Intelligent Vehicles 95, Detroit, MI*, vol. pp, pp. 54–59.

27. N. Apostoloff and a. Zelinsky, "Robust vision based lane tracking using multiple cues and particle filtering," *IEEE IV2003 Intelligent Vehicles Symposium. Proceedings (Cat. No.03TH8683)*, no. Figure 2, pp. 558–563, 1999.

28. F. Paetzold and U. Franke, "Road Recognition in Urban Environment," *Source*, pp. 87–91, 1998.

29. J. C. Mccall and M. M. Trivedi, "An Integrated , Robust Approach to Lane Mark-

ing Detection and Lane Tracking," *System*, no. June, 2004.

30. J. P. Gonzalez and U. Ozguner, "Lane detection using histogram-based segmentation and decision trees," *in Proc. IEEE Intell. Transp. Syst., Oct*, pp. 346–351, 2000.

31. Y. Wang, "Lane detection and tracking using B-Snake," *Image and Vision Computing*, vol. 22, no. 4, pp. 269–280, 2004.

32. A. Lopez, J. Serrat, C. Canero, and F. Lumbreras, "Robust Lane Lines Detection and Quantitative Assessment," in *IbPRIA 2007*, no. section 2, pp. 274–281, Springer-Verlag, 2007.

33. D. Pomerleau, "RALPH: Rapidly adapting lateral position handler," *IEEE Symposium on Intelligent Vehicles*, vol. 7, no. 1, pp. 506–511, 1995.

34. J. Kosecka, R. Blasi, C. J. Taylor, and J. Malik, "A Comparative Study of Vision-Based Lateral Control Strategies for Autonomous Highway Driving," *Int. J. Robot Res.*, vol. 18, no. 15, pp. 442–453, 1999.

35. Z. Tan, "Vision Based Lane Detection in Autonomous Vehicle," *Transportation*, pp. 5258–5260, 2004.

36. H. R. Johnson Eric, "Computer Vision Class Project," 2007.

37. M. Zuliani, "RANSAC Toolbox for Matlab," 2008.

38. T. Veit, J.-P. Tarel, P. Nicolle, and P. Charbonnier, "ROad MArking Database, http://www.lcpc.fr/en/produits/ride ."